Inverse regulation of secretion and inflammation in human airway gland serous cells by neuropeptides upregulated in allergy and asthma

Derek B. McMahon,[1] Michael A. Kohanski,[1] Charles C.L. Tong,[1] Peter Papagiannopoulos,[1] Nithin D. Adappa,[1] James N. Palmer,[1] and Robert J. Lee[1,2,*]

[1]Department of Otorhinolaryngology and [2]Department of Physiology, University of Pennsylvania Perelman School of Medicine, Philadelphia, PA USA

*Correspondence to

Robert J. Lee

Hospital of the University of Pennsylvania

Department of ORL-HNS

3400 Spruce Street,

5th floor Ravdin, Suite A

Philadelphia, PA 19104

(t) 215-573-9766

(e) rjl@pennmedicine.upenn.edu

Conflict of Interest Statement: The authors declare that no conflicts of interest exist.

ABSTRACT

Airway submucosal gland serous cells are sites of expression of the cystic fibrosis transmembrane conductance regulator (CFTR) and are important for fluid secretion in conducting airways from the nose down to small bronchi. We tested if serous cells from human nasal turbinate glands secrete bicarbonate (HCO_3^-), important for mucus polymerization, during stimulation with the cAMP-elevating agonist vasoactive intestinal peptide (VIP) and if this requires CFTR. Isoalted serous cells stimulated with VIP exhibited a ~20% cAMP-dependent decrease in cell volume and a ~0.15 unit decrease in intracellular pH (pH_i), reflecting activation of Cl^- and HCO_3^- secretion, respectively. Pharmacology, ion substitution, and studies using cells from CF patients suggest serous cell HCO_3^- secretion is mediated by conductive efflux directly through CFTR. Interestingly, we found that neuropeptide Y (NPY) reduced VIP-evoked secretion by blunting cAMP increases and reducing CFTR activation through G_i-coupled NPY1R. Culture of primary gland serous cells in a model that maintained a serous phenotype confirmed the activating and inhibiting effects of VIP and NPY, respectively, on fluid and HCO_3^- secretion. Moreover, VIP enhanced secretion of antimicrobial peptides and antimicrobial efficacy of gland secretions while NPY reduced antimicrobial secretions. In contrast, NPY enhanced the release of cytokines during inflammatory stimuli while VIP reduced cytokine release through a mechanism requiring CFTR conductance. As levels of VIP and NPY are up-regulated in disease like allergy, asthma, and chronic rhinosinusitis, the balance of these two peptides in the airway may control airway mucus rheology and inflammatory responses through gland serous cells.

INTRODUCTION

Several distinct obstructive airway diseases share a phenotype of thickened mucus and/or mucostasis, including chronic rhinosinusitis (CRS) (1), cystic fibrosis (CF), asthma (2, 3), and COPD (4). In conducting airways from the nasal turbinates down to small bronchi ~1 mm^2 in diameter, a large percentage of airway surface liquid (ASL) and mucus is generated in airway submucosal exocrine glands (5-7). Submucosal gland serous acinar cells are sites of expression of the cystic fibrosis (CF) transmembrane conductance regulator (CFTR) Cl^- channel (8-12). Defects in CFTR-dependent serous cell secretion likely play an important role in CF pathology, supported by observations of occluded mucus-filled gland ducts, gland hypertrophy and hyperplasia, and gland infection in lungs of CF patients (13, 14). Intact glands from CF individuals or transgenic CF animals secrete less fluid in response to cAMP-elevating agonists such as vasoactive intestinal peptide (VIP) (15-24) compared with non-CF glands. Gland hypertrophy, duct plugging, and/or excess mucus secretion have also been observed in COPD and asthma (4, 25-35), with gland hypertrophy being greater in fatal asthma cases than non-fatal cases (33).

Proper gland secretion likely requires bicarbonate (HCO_3^-) secretion by serous cells at the distal ends of the glands to facilitate polymerization of mucins secreted by more proximal mucous cells (36-41) (**Figure 1A**). However, the mechanisms by which serous cells secrete HCO_3^- are unknown. HCO_3^- may also be critical to the efficacy of antimicrobial peptides secreted by serous cells (42-45), including lysozyme, lactoferrin, LL-37, and Muc7 (46). Understanding how airway glands secrete HCO_3^- may yield insights into the pathophysiology of CRS, CF, COPD, and asthma, all of which have a common phenotype of altered airway mucus secretion or rheology.

We previously developed live cell imaging techniques to study living primary mouse nasal serous cells and demonstrated that they secrete HCO_3^- during cholinergic stimulation (47). Cholinergic-induced secretion is largely intact in CF (10-12, 15-24, 46-48), as it is mediated by Ca^{2+} activated Cl^- channels, including TMEM16A (12). An initial goal of the current study was to directly test if serous acinar cells secrete HCO_3^- during stimulation with VIP, whether this occurs through CFTR, and if activation of

TMEM16A could substitute. A further goal was to understand the potential relationship of VIP and neuropeptide Y (NPY), both upregulated in inflammatory airway diseases, in control and composition of airway gland secretions. A recent review highlighted a need for a clearer portrait of neuropeptide regulation of submucosal gland secretion within the context of the diverse lung diseases characterized by mucus obstruction (49).

Parasympathetic VIPergic neurons (50-55) and NPY-containing fibers (56-58) are exist in the respiratory tract, with some nerves co-expressing VIP and NPY (59), including in the proximity of submucosal glands (60, 61). Immune cells like activated macrophages (62-64) or epithelial cells (65) can also make NPY. Elevated NPY in allergic asthma (66, 67) may link psychological stress with asthma exacerbations (68-70). Both VIP-containing and NPY-containing nerves may be increased in mucosa from patients with allergic rhinitis (71, 72) or irritative toxic rhinitis (73). VIP and NPY, but not substance P or calcitonin gene-related peptide (CGRP), are found in the pedicle of nasal polyps, suggesting they may play a role in polyp formation (74). Mice lacking NPY or NPY1R have reduced allergic airway inflammation (75), suggesting this neuropeptide and this receptor isoform detrimentally contribute to inflammatory airway diseases. One study found NPY and NPYR1 expression elevated in mouse lungs after influenza infection; knockout of NPY reduced the severity of disease and lowered IL-6 levels (63). In other studies outside the airway, NPY deficiency can reduce Th2 responses (76, 77).

The role of VIP as a cAMP-dependent activator of gland secretion has been extensively studied (11, 19, 78), but the role of NPY is less clear. A cocktail of NPY and norepinephrine inhibited cultured tracheal gland cell glycoprotein secretion (79), and NPY inhibits bulk mucus secretion in ferret trachea (80), though there is little mechanistic data for how NPY affects epithelial or gland cells specifically. We sought to understand how VIP and NPY signaling may interact to control of gland serous cell secretion. Because NPY receptors are often G_i-coupled, they may reduce cAMP-evoked responses to G_s-coupled VIP or beta-adrenergic receptors (81-83) or CCK receptors (84). We hypothesized that NPY may reduce airway serous cell fluid and/or HCO_3^- secretion during VIPergic stimulation though modulation of cAMP and thus CFTR. Moreover, VIP and NPY are potent immunomodulators in the gut (85). These peptides

may be relevant for airway gland-cell-driven inflammation which may help drive airway submucosal remodeling or airway inflammation.

We examined the effects of VIP and NPY on secretion from primary human airway gland serous acinar cells isolated from nasal turbinate. Cells were studied acutely as well as in an air-liquid interface (ALI) culture model that retained expression of important serous cell markers and facilitated polarized studies and co-culture with human immune cells. Results below contribute to our understanding of airway serous cell secretion and the role of CFTR in both secretion and inflammation, also suggesting therapeutic strategies (NPY1R antagonists, TMEM16A activators) for obstructive inflammatory airway diseases.

RESULTS

VIP stimulates both Cl^- and HCO_3^- secretion from airway gland serous cells through CFTR

Submucosal gland acini and single acinar cells (**Figure 1B**) were isolated from human nasal middle turbinate as previously described (11). Serous acini exhibited secretory-granule localized immunofluorescence for serous cell marker lysozyme (**Figure 1C**; as previously reported (10, 12, 48)) as well as basolateral immunofluorescence of VIP receptors VIPR1 (VPAC1; **Figure 1D**) and VIPR2 (VPAC2; **Figure 1E**). In contrast, secretory Cl^- channels TMEM16A and CFTR exhibited apical membrane immunofluorescence (**Figure 1F-G**), as previously observed (10, 12, 48).

Fluid and ion transport pathways were studied in acutely isolated serous cells using simultaneous DIC measurement of cell volume and quantitative fluorescence microscopy of ion indicator dyes to measure the concentrations of ions involved in driving fluid secretion (Cl^-/HCO_3^-), a technique pioneered in the study of parotid gland secretory acinar cells (86, 87) and adapted previously for airway gland serous cells (10-12, 46-48). Epithelial fluid secretion is driven largely by Cl^-. Acinar cell shrinkage during agonist stimulation reflects efflux of cellular K^+ and Cl^- upon activation of secretion and movement of osmotically obliged water. Cell swelling upon removal of agonist reflects solute uptake via mechanisms that sustain secretion such as the bumetanide-sensitive $Na^+K^+2Cl^-$ co-transporter NKCC1 (46) (**Figure 2A**). Human nasal serous cells shrank by approximately 20% when stimulated with the cAMP-elevating agonists forskolin or VIP (**Figure 2B**), as we previously reported (11). We now found this was also accompanied by a transient decrease in intracellular pH (pH_i) followed by a more sustained increase in pH_i (**Figure 2C-D**).

Both the cell shrinkage and decrease in pH_i were absent in cells isolated from CF patients (**Figure 2C-D**). The agonist-evoked pH_i decrease was absent when HCO_3^- was removed from the media (**Supplemental Figure 1A-C**), and the secondary pH_i increase was blocked with inhibition of the $Na^+HCO_3^-$ co-transporter (NBC; **Supplemental Figure 1D**). This suggests the transient pH_i decrease reflects HCO_3^- efflux during activation of secretion, while the pH_i increase reflects activation of NBC, sustaining HCO_3^- secretion by keeping intracellular HCO_3^- high. This is similar to cholinergic evoked pH_i

decreases and subsequent elevation of pH_i by Na^+/H^+ exchangers (NHEs) in mouse nasal serous cells (47), but reveals an important mechanistic difference between cAMP and Ca^{2+} pathways.

The pH_i decrease was also blocked by eliminating the driving forces for HCO_3^- efflux using ion substitution (**Supplemental Figure 1E**), suggesting the pH_i decrease is mediated by conductive HCO_3^- efflux, such as an ion channel. Both forskolin-induced pH_i decrease and cell volume decrease were inhibited by $CFTR_{inh}172$ (10 μM; **Figure 2E**). VIP-induced cell volume and pH_i decreases were blocked by $CFTR_{inh}172$ or K^+ channel inhibitors clofilium and clotrimazole (30 μM each; **Figure 2F**) demonstrating a requirement for both CFTR and conductive counterion K^+ efflux, supporting a Cl^- channel as the HCO_3^- efflux pathway. VIP-evoked responses were not blocked by the calcium-activated Cl^- channel inhibitors niflumic acid (100 μM), $T16A_{inh}$-A01 (10 μM), $CaCC_{inh}$-A01 (10 μM) or 4,4'-Diisothiocyanostilbene-2-2"-disulfonic acid; (DIDS; 1 mM) (**Figure 2F**). These data suggest that VIP receptor activation or direct cAMP elevation with forskolin can activate both Cl^- and HCO_3^- secretion directly through CFTR. We found no evidence for Cl^-/HCO_3^- exchanger-mediated HCO_3^- efflux in primary serous cells (**Supplemental Figure 2**), suggesting CFTR is the main HCO_3^- efflux pathway during cAMP stimulation, agreeing with recent Calu-3 studies suggesting CFTR sustains HCO_3^- secretion (88, 89) instead of the pendrin Cl^-/HCO_3^- exchanger (90, 91).

In contrast, cholinergic agonist carbachol (CCh; 10 μM), which activates Ca^{2+}-driven TMEM16A-mediated secretion (10-12, 46), stimulated cell shrinkage and pH_i decreases that were blocked by TMEM16A inhibitors NFA, $T16A_{inh}$-A01, $CaCC_{inh}$-A01 (**Figure 2G**). CCh-induced responses were intact in cells from CF patients (**Figure 2H**). Activation of TMEM16A with a pharmacological activator (E_{act}; 25 μM) was sufficient to restore both Cl^- (shrinkage) and HCO_3^- (pH_i) secretion responses to VIP in cells from CF patients (**Figure 2H**). In summary, our data suggest serous cell shrinkage during VIP stimulation reflects secretion of both Cl- and HCO3- directly through CFTR (**Figure 2I**).

NPY reduces CFTR-mediated serous cell fluid and HCO_3^- secretion during VIP stimulation

Beyond the histological observations described above regarding NPY in airways, we also noted that Calu-3 cells, a bronchial adenocarcinoma line frequently used as a serous cell surrogate due to high

CFTR and lysozyme expression, express relatively high amounts of NPY1R relative to other airway cancer lines according to public gene expression databases (**Supplemental Tables 1 and 2**). This may be an artifact of Calu-3 cells being cancer cells, but we decided to test for NPY receptor function in primary serous cells.

We observed no secretory responses to 100 nM NPY (**Figure 3A**), but the magnitude of VIP-evoked pH_i decreases and cell shrinkage were reduced after NPY (**Figure 3A-B**). As a control, a scrambled NPY peptide had no effect (**Figure 3B**). We hypothesized that G_i-coupled NPY receptors might blunt the magnitude of VIP-evoked cAMP increases, thus reducing Cl^- and HCO_3^- efflux through CFTR. We measured cellular Cl^- permeability using 6-methoxy-N-(3-sulfopropyl)quinolinium (SPQ), a dye quenched by Cl^- but not by NO_3^- (48, 92). Substitution of extracellular Cl^- for NO_3^- results in electroneutral influx of NO_3^- and efflux of Cl^-, causing a decrease in intracellular $[Cl^-]$ ($[Cl^-]_i$) and increase in intracellular SPQ fluorescence. Because most Cl^- channels are nearly equally permeable to Cl^- and NO_3^-, the rate of fluorescence increase is roughly equivalent to the anion permeability (93). In the presence of VIP, SPQ fluorescence rapidly increased upon NO_3^- substitution. This was reduced by half in cells stimulated in the presence of 100 nM NPY but not 100 nM scrambled NPY (**Figure 3C-D**). In the presence of $CFTR_{inh}172$, anion permeability was markedly reduced and NPY had no effects (**Figure 3D**), suggesting that NPY directly reduces VIP-stimulated CFTR permeability.

CFTR is activated by PKA downstream of cAMP. We imaged cAMP changes in nasal serous cells in real time using a fluorescent mNeonGreen-based cAMP biosensor (cADDis (94)). 1 μM VIP induced a rapid and reversible increase in cAMP (decrease in cADDis fluorescence) that was blocked by VIPR antagonist VIP_{6-28} (1 μM; **Figure 4A-B**). The cAMP increase was independent of Ca^{2+}, as it was not blocked by intracellular and extracellular calcium chelation (**Figure 4C**). Interestingly, we also found no differences in the ability of VIP to increase cAMP in Wt or CF cells (**Supplemental Figure 3**), in contrast to previous hypotheses that cAMP signaling may be defective in CF cells (95). However, NPY (100 nM) significantly reduced the cAMP responses to 0.5 μM and 5 μM VIP (**Figure 4D-E**); the effects of NPY were eliminated in the presence of a NPY1R antagonist BIBO 3304 (5 μM) or in cells treated with pertussis toxin (PTX), which ADP-ribosylates and inactivates G_i proteins (**Figure 4D-E**). These data

demonstrate that NPY reduces cellular anion efflux through CFTR to blunt Cl^-, HCO_3^-, and fluid secretion from these cells.

To facilitate polarized studies of serous cells, we used previously published culture methods for gland acinar cells that preserve a serous phenotype (96-98). Serous cells cultured at air liquid interface (ALI) expressed serous marker Muc7 (99), VIP1R, and VIP2R by Western (**Figure 5A**). Mucous maker Muc5B was not detected (**Figure 5A**). Serous cell markers lysozyme (100, 101), Muc7, and VIPR1 and VIPR2 were detected by immunofluorescence (**Figure 5B-C**). Many of these same markers were detected in Calu-3 cells (**Supplemental Figure 4-5**). We used ELISAs to confirm that serous cell cultures expressed serous cell Muc7 but not goblet cell mucin Muc5AC or mucous cell mucin Muc5B (**Supplemental Figure 6**).

Serous cell ALIs also expressed functional apical CFTR; when ALIs were loaded with SPQ, apical substitution of Cl^- for NO_3^- led to a decrease in $[Cl^-]_i$ (increase in SPQ fluorescence) that was enhanced by VIP (1 μM), blocked by $CFTR_{inh}172$ (10 μM), and blunted in the presence of NPY (100 nM; **Figure 6A**). Similar to studies of freshly isolated cells above, TMEM16A inhibitors did not affect VIP-activated Cl^- permeability (**Figure 6A**). ALIs were resistant to viral expression of cADDis, but we measured changes in steady-state cAMP levels 5 min after stimulation with VIP ± NPY. NPY reduced cAMP increases in response to VIP or isoproterenol, and this was abrogated by PTX (**Figure 6B**), suggesting effects of NPY on cAMP are dependent on activation of G_i-coupled receptors.

Airway surface liquid (ASL) was labeled with Texas red dextran and imaged with confocal microscopy to track fluid secretion in serous cell ALIs stimulated VIP (1 μM) ± NPY (100 nM) on the basolateral side. VIP increased ASL height, and this was inhibited by NKCC1 inhibitor bumetanide (100 μM), PKA inhibitor H89 (10 μM), or VIPR antagonist $VIP_{(6-28)}$ (1 μM) (**Figure 6C-D**). NPY, but not scrambled NPY, inhibited VIP-induced secretion (**Figure 6C-D**). Ca^{2+}-driven 100 μM CCh-induced secretion was unaffected by NPY (**Figure 6D**), while effects of another cAMP-elevating agonist, isoproterenol, was inhibited by NPY (**Figure 6D**), showing effects of NPY were specific for cAMP-elevating agonists.

Primary human monocyte-derived macrophages (MΦs) stimulated with PKC-activating phorbol myristate acetate (PMA; 100 nM for 48 hrs) produce NPY ((62) and **Supplemental Figure 7**), were washed to remove PMA and incubated for 24 hours in a 24 well plate. Serous cells on transwells were then transferred into the same plates above the MΦs in the 24 hour conditioned media on the basolateral side. Addition of VIP (2 μM) caused an increase in ASL height that was reduced in the presence of PMA-stimulated MΦs compared with unstimulated MΦs (**Figure 6E**). In the presence of PMA-stimulated MΦs, VIP-induced fluid secretion was increased by addition of NPY1R antagonist BIBO 3304 (1 μM).

ASL was labeled with SNARF-1-dextran, a pH probe with ratiometric emission (580 and 650 nm) and thus insensitive to changes in volume. SNARF-1-dextran was sonicated in perfluorocarbon, allowing measurement of pH within the physiological ASL with no addition of extra fluid (102). Steady-state unstimulated ASL pH was 7.2 ± 0.04, equivalent to a $[HCO_3^-]$ of 15 mM by Henderson-Hasselbach with 5% CO_2 ($[HCO_3^-]_i = 1.2\ mM \times 10^{pH-6.1}$). ASL pH was reduced to 6.9 ± 0.06 (equivalent to 7.6 mM HCO_3^-) by NBC inhibitor 4,4'-dinitrostilbene-2,2'-disulfonic acid (DNDS; 30 μM) but was not significantly reduced with NPY (100 nM) (**Figure 6F**). VIP (1 μM) increased ASL pH to 7.6 ± 0.04 (equivalent to 38 mM HCO_3^-), suggesting VIP stimulated HCO_3^- secretion. VIP-increased ASL pH was reduced by NPY (7.3 ± 0.05) or DNDS (7.1 ± 0.03). Effects of NPY were blocked by PTX. NPY had similar inhibitory effects on ASL pH increases with forskolin and isoproterenol (**Figure 6F**). Note that with increase in ASL volume (**Figure 6C**) as well as buffering capacity, the amount of secreted HCO_3^- would be even greater than predicted changes in $[HCO_3^-]$.

Serous cell ALIs were incubated in the presence of unstimulated or PMA-stimulated MΦs as above and ASL pH was measured 2 hours later. ASL pH was not different in the presence or absence of unstimulated MΦs, but PMA-stimulated MΦs reduced steady-state ASL pH (**Figure 6G**). This effect was inhibited by an NPY1R antagonist (BIBO 3304; 1 μM) and pH was also increased by addition of VIP (1 μM) (**Figure 6G**). Effects of NPY on HCO_3^- secretion were verified using a real-time HCO_3^- secretion assay using larger apical volumes of SNARF-1-dextran, which confirmed secretion was dependent on apical CFTR (**Supplemental Figure 8**).

NPY inhibits VIP-evoked increases in serous cell antimicrobial peptide secretion

Serous cells secrete a variety of antimicrobial peptides, and secretion can involve cAMP. It is likely that the same stimuli that activate fluid secretion likely activate protein secretion, which is also driven by Ca^{2+} and cAMP (103, 104). To test if NPY can reduce VIP-induced secretion of antimicrobials, we measured secreted levels of lysozyme, Muc7, and β-defensin 1 (hβD1). Cells were stimulated basolaterally with forskolin (5 μM) or VIP (1 μM) in the presence or absence of NPY or scrambled NPY (100 nM). Forskolin and VIP both increased secretion of lysozyme, Muc7, and βD1, and this was reduced by NPY (**Figure 7A**).

VIP increases bactericidal activity of serous cell secretions while NPY reduces it

Carbonate and/or HCO_3^- has been reported to enhance antimicrobial activity of airway antimicrobial secretions (45, 105). We did observe a small effect of HCO_3^- on antimicrobial activity of secretions produced by Calu-3 bronchial serous-like cells (**Supplemental Figure 9**). However, we hypothesized that NPY might have more profound effects on antimicrobial activity through inhibition of both HCO_3^- secretion and antimicrobial peptide secretion. We tested the anti-bacterial efficacy of apical washings of serous cells stimulated with VIP ± NPY or scrambled NPY. VIP increased the antibacterial effects of ASL washings (as measured by CFU counting) against both clinical isolates of gram negative *P. aeruginosa* (**Figure 7B**) and methicillin resistant gram positive *S. aureus* (MRSA; **Figure 7C**), fitting with data above suggesting increased antimicrobial peptide secretion. Addition of NPY itself had no effect, but NPY substantially blunted the effect of VIP against either species of bacteria (**Figure 7B-C**). Scrambed NPY did not reduce the increased efficacy observed with VIP (**Figure 7B-C**). A fluorescent live-dead assay (Syto9 and propidium iodide staining) confirmed reduced efficacy of NPY+VIP stimulated ASL after only 5 min incubation with *P. aeruginosa* (**Supplemental Figure 10**).

NPY has pro-inflammatory effects in primary serous acinar cells

Both VIP and NPY have immunomodulatory roles in many tissues (106-109), including VIP having anti-inflammatory or protective effects in parotid acini (106, 110-113) and NPY having pro-inflammatory effects in leukocytes (85). Acinar cells from parotid and pancreatic exocrine glands can make and release cytokines (114-117). Infection of isolated human tracheal submucosal gland cells with rhinovirus, which can activate TLR3 (118), increases IL-1α, IL-1β, IL-6, and IL-8 (119). TLR4 is also expressed in pig tracheal acinar cells (120), and submucosal TLR4 levels may be elevated in CF (121). We hypothesized that airway gland cells may be an overlooked significant contributor to the airway cytokine milieu, and this may be modulated by VIP and/or NPY.

In primary nasal serous cell ALIs, the TLR4 activator lipopolysaccharide (LPS) and TLR3 activator poly(I:C) induced secretion of IL-6, TNFα, IL-1β, and granulocyte macrophage colony stimulating factor (GMCSF (**Supplemental Figure 11**). TLR2 activator lipotechoic acid (LTA) also increased secretion of IL-6 and TNFα, while TNFα itself increased secretion of IL-1β and GM-CSF (**Supplemental Figure 11**). Furthermore, a type 2 inflammatory cocktail of IL-4 and IL-13 (122) also increased secretion of GM-CSF (**Supplemental Figure 11**). Airway gland serous cells can thus respond to and secrete a variety of inflammatory cytokines.

While NPY or VIP had no effect alone on IL-6, TNFα, or GMCSF, NPY increased IL-1β production ~2-fold and significantly increased cytokine production (~50%) during LPS, LTA, IL-4+IL-13, and TNF-α (**Supplemental Figure 11)** stimulation. Effects of NPY were blocked by pertussis toxin, implicating a GPCR G_i-coupled pathway. In contrast, VIP slightly reduced cytokine secretion (25-50%) when combined with inflammatory stimuli, while these reductions were eliminated in the presence of NPY (**Supplemental Figure 11**). Together, these data suggest that VIP has a small anti-inflammatory effect while NPY is pro-inflammatory when combined with a broad range of stimuli.

A strong Th2 environment by itself may increase other inflammatory responses in airway cells (123). Co-stimulation with IL-4+IL-13 increased IL-6 and GM-CSF secretion in response to either poly(I:C) or LPS, and this was enhanced further in the presence of NPY (**Supplemental Figure 12A**), suggesting that NPY is pro-inflammatory even within the context of elevated IL-4 and IL-13 in

inflammatory airway diseases. To validate results from cultured cells, we incubated freshly dissociated primary serous celsl seeded at high density with TNFα or poly(I:C) ± NPY or scrambled NPY for 18 hours. TNFα and poly(I:C) increased secretion IL-33, GM-CSF, or IL-6, and this was enhanced by NPY but not scrambled NPY (**Supplemental Figure 12B**), supporting that airway gland serous cells can secrete several cytokines involved in allergy, asthma, and chronic rhinosinusitis, and confirming NPY is pro-inflammatory.

We examined cytokine release in response to heat-killed clinical CRS isolates of gram negative *P. aeruginosa* and gram positive methicillin-resistant *Staphylococcus aureus* (MRSA). Incubation of serous cell ALIs with either species of bacteria increased secretion of IL-6, GM-CSF, and TNFα (**Figure 8**). NPY (100 nM), but not scrambled NPY, significantly increased cytokine release, supporting that NPY has pro-inflammatory effects during airway infections.

Anti-inflammatory effects of VIP require apical functional CFTR conductance, but activation of TMEM16A can substitute for CFTR.

In airway cells, Cl^- conductance has been suggested to be anti-inflammatory (124, 125), with increased intracellular $[Cl^-]_i$ promoting inflammation (126). In serous cells stimulated with VIP, $[Cl^-]_i$ may be higher if there is a lack of apical CFTR efflux pathway in CF patients. To test if CFTR was required for anti-inflammatory effects observed with VIP, we first stimulated serous cell ALIs with NPY, which increased IL-1β secretion; NPY-induced IL-1β was not altered by $CFTR_{inh}172$ or activation of TMEM16A (E_{act}) (**Figure 9A**). However, VIP reduced IL-1β secretion by >50% (**Figure 9A**). $CFTR_{inh}172$ reversed the anti-inflammatory effect of VIP, while adding E_{act} restored the anti-inflammatory effect of VIP (**Figure 9A**). The effect of E_{act} reversed with $CaCC_{inh}$-A01 (**Figure 9A**). These data suggest that CFTR is required for the anti-inflammatory effects of VIP but TMEM16A can substitute. However, the Cl^- conductance itself is not sufficient, as E_{act} did not have anti-inflammatory effects in the absence of VIP. This may be because a reduction in $[Cl^-]_i$ would require counter-ion (K^+) flux that would be activated downstream of a cAMP-secretagogue like VIP, as we have previously suggested through cAMP-

activated Ca^{2+} signals (11), but not during direct activation of TMEM16A with apical E_{act}. We saw similar results when serous cells were stimulated with heat-killed *P. aeruginosa*. VIP reduced GM-CSF and IL-6 secretion, but these effects were blocked by $CFTR_{inh}172$ and subsequently restored by E_{act} (**Figure 9B**). $CFTR_{inh}172$ and E_{act} had no effect alone on *P. aeruginosa*-induced GM-CSF or IL-6 secretion (**Figure 9B**), again suggesting that an apical Cl^- conductance is necessary, but not sufficient, for anti-inflammatory effects of VIP.

DISCUSSION

This paper reveals several important insights into airway gland serous cell physiology. First, we directly demonstrate that serous cells secrete HCO_3^- in addition to Cl^- during VIPergic stimulation. Our experiments suggest this is conductive HCO_3^- efflux through CFTR with little contribution from Cl^-/HCO_3^- exchangers such as pendrin. We found no defect in cAMP signaling in primary serous cells, supporting that appropriate pharmacological correction of mutant CFTR function (127) would restore fluid secretion in response to appropriate physiological stimuli (e.g., VIP). However, in patients that cannot benefit from CFTR correction (e.g., those with a premature stop code-on mutation), our data suggest activation of TMEM16A, bypassing CFTR, is sufficient to restore HCO_3^- efflux during VIP stimulation in CF serous cells (128).

We also demonstrate a novel inverse relationship between NPY and VIP in the regulation of serous cell secretion. Our data here suggest that VIP may promote watery secretions of glands through elevated fluid and HCO_3^- secretion to thin mucus. However, we hypothesize that under conditions of increased NPY (e.g., in asthma), the ability of VIP to stimulate fluid and HCO_3^- secretion is markedly impaired, as is the secretion of antimicrobial peptides. Coupled with increased inflammation in the presence of NPY, our data suggest NPY may have multiple detrimental effects in diseases of mucus thickening/mucostasis. We (129) and others (130-132) have shown that NPY decreases airway ciliary beat frequency, which may further impair mucociliary clearance.

Patients challenged with allergens produce nasal secretions that have detectible levels of VIP (31, 32), suggesting this peptide is released in large amounts during the airway allergic response, possibly through histamine activation of sensory neurons (37). Allergic rhinitis patients may have a higher density of sinonasal VIPergic fibers (21, 22, 33-35), increased VIP receptor expression (36), and baseline nasal secretions with elevated concentrations of VIP compared with control individuals (32). This may thin out mucus by increasing secretion of HCO_3^- and fluid from gland serous cells. In contrast, elevations of NPY may thicken mucus in some asthma patients, with the balance of these two peptides contributing toward setting airway mucus rheology. We hypothesize that in some asthma, COPD, or

CRS patients, NPYR1 antagonists may be useful that to thin secreted mucus, enhance antimicrobial secretion, and reduce inflammatory responses from gland acini by relieving repression of VIP-induced signaling.

The important contribution of exocrine acinar cells to inflammation is already established in parotid and pancreatic acini within the context of Sjögren's syndrome and pancreatitis, respectively (114-116). However, this has been largely unstudied in the airway. In bronchi, gland volume may be up to 50-fold larger than the volume of surface goblet cells (5, 6, 133-135). Gland acini are likely significant contributors to the airway cytokine milieu, particularly when barrier dysfunction occurs during chronic inflammation in CRS, COPD, asthma, or CF (136-138) and/or when gland hypertrophy and hyperplasia occur during COPD and asthma (25, 27, 28, 30). Elevations of NPY may alter submucosal gland function by both reducing cAMP-driven CFTR-mediated secretion as well as enhancing production of cytokines like GM-CSF and IL-1β that are important in allergic inflammation (139-142), airway neutrophil or eosinophil infiltration (143, 144), and Th2 polarization (145-147). NPY by itself increase IL-1β secretion, and IL-1β polymorphisms may contribute to CF (148) or CRS (149); it remains to be determined if these polymorphisms relate to expression or secretion of IL-1β from gland acini. Regardless, NPY-increased serous cell-derived cytokines likely help to drive inflammation.

Finally, our data support previous observations (124, 125) that the Cl^- channel activity of CFTR is anti-inflammatory during VIP stimulation. A loss of these anti-inflammatory effects of VIP in CF patients lacking functional CFTR may contribute to the hyperinflammatory phenotypes reported (150). As we saw for Cl^- and HCO_3^- secretion, our data suggest that activation of TMEM16A can also compensate for loss of CFTR to restore anti-inflammatory effects of VIP, suggesting another possible benefit to targeting TMEM16A in CF submucosal glands of patients who cannot benefit from CFTR potentiator and/or corrector therapies due to CFTR genotype.

METHODS

Experimental Procedures

Isolation of primary serous acinar cells, immunofluorescence, and live cell imaging of acinar cell volume, pH_i (SNARF-5F), and Cl^- (SPQ) was carried out as described (10-12, 47, 48). ASL height and pH measurements and ELISAs were carried out as previously reported (92, 129, 151-157). Bacterial growth assays were carried out as previously described (158, 159). More detailed methods for all procedures as well as specific reagents used are provided in the **Supplemental Materials**.

Study Approval

Tissue was acquired with IRB approval (University of Pennsylvania protocol # 800614) in accordance with the University of Pennsylvania School of Medicine guidelines regarding residual clinical material in research, the United States Department of Health and Human Services code of federal regulations Title 45 CFR 46.116, and the Declaration of Helsinki.

Serous cell isolation and culture

Primary human nasal serous acinar cells were used to study Cl^-/fluid and HCO_3^- secretion. Studies of human turbinate submucosal gland serous cells are directly relevant to the understanding of mechanisms of CRS, particularly CF-related CRS (160), and turbinate gland serous cells approximate gland serous cells from the lower airway. Histology suggests that nasal airway glands are similar to tracheal/bronchial glands (161), and we have established that pig bronchial serous cell responses are identical to human turbinate serous cells (11, 12). Working with human cells has important advantages over mice, as data from intact glands (19, 162, 163) and our own studies (10-12, 46-48) have established important differences between mouse serous cells and those from pigs and humans.

Patients undergoing medically indicated sinonasal surgery were recruited from the Department of Otorhinolaryngology at the University of Pennsylvania with written informed consent as previously described (151-154). Inclusion criteria were patients ≥18 years of age undergoing surgery for sinonasal

disease (CRS) or other procedures (e.g., trans-nasal approaches to the skull base) where tissue was classified as "control." Exclusion criteria included history of systemic inheritable disease (e.g., granulomatosis with polyangiitis or systemic immunodeficiencies) with the exception of cystic fibrosis (CF). Members of vulnerable populations were not included.

Comparisons made here between non-CF and CF cell Cl^- and HCO_3^- secretion are valid because SNARF and SPQ properties were identical between CF and non-CF cells, and both genotypes had identical resting $[Cl^-]_i$, resting pH_i, and intracellular pH_i buffering capacity (**Supplemental Figures 13-14**).

For culturing, acinar cells were washed with and resuspended in 1:1 MEME plus 20% FBS, 1x pen/strep, gentamycin (100 µg/ml), and amphotericin B (2.5 µg/ml) as described by Finkbeiner (96). Cells were seeded (~$3x10^5$ cells per cm^2) on transparent Falcon filters (#353095; 0.3 cm^2; 0.4 µm pores) coated with human placental collagen. After confluence, the media was changed to MEME + Lonza bronchial epithelial cell culture supplements (5 µg/ml insulin, 5 µg/ml transferrin, 0.5 µg/ml hydrocortisone, 20 ng/ml triiodothyronine, 20 nM retinoic acid, 2 mg/ml BSA) but not EGF, with 2% NuSerum. Media lacking EGF combined with the plastic type of these transwell filters was previously shown to differentiate cells into a serous phenotype (96, 164). After 5 days of confluence, TEER reached ~300 - 500 Ω•cm^2 and cells were fed with the media above lacking NuSerum on the basolateral side while the apical side was washed with PBS and exposed to air. Cells were used after 2-4 weeks at air-liquid interface.

Imaging of intracellular cAMP dynamics in isolated nasal gland serous cells

Isolated acinar cells were plated for 30 min on glass coverslips, followed by washing and addition of serum-free Ham's F12K (Gibco) containing cADDis expressing BacMam (Montana Molecular) plus 5 mM NaButyrate to enhance expression. Cells were imaged after 24 hrs incubation at 37 °C. A BacMam vector was previously used to express proteins in lacrimal gland acinar cells (165-167). Cells were imaged as above under CO_2/HCO_3^- conditions using a standard GFP/FITC filter set (Semrock) on a Nikon microscope (20x 0.75 Plan Apo objective) equipped with a QImaging Retiga R1 camera and XCite 110 LED illumination system. Data were acquired with Micromanager (168). Experiments were done

under ion substitution conditions (high K^+) to reduce volume changes as previously described (10-12, 47, 48) to ensure that cADDis fluorescence changes were not artifacts of cell volume change during activation of secretion, confirmed by pilot experiments using mNeonGreen-only BacMam. For experiments with pertussis toxin (PTX), PTX was included with the BacMam virus infection reaction (~24 hours pretreatment).

Primary culture of human monocyte-derived macrophages (Mϕs)

Monocytes were isolated from healthy apheresis donors by RosetteSep™ Human Monocyte Enrichment Cocktail (Stem Cell Technologies) by the University of Pennsylvania Human Immunology Core and provided as de-identified untraceable cells. Monocytes were differentiated into macrophages by 10 days of adherence culture in high glucose RPMI media containing 10% human serum. Differentiation to Mϕs was confirmed by functional expression of markers including histamine H1 receptors (169, 170) determined by Ca^{2+} imaging (**Supplemental Figure 15**) with specific antagonists as well as secretion of appropriate cytokines in response to M1 vs M2 polarization stimuli (**Supplemental Figure 7**).

Statistics

Numerical data was analyzed in Microsoft Excel or GraphPad Prism. Statistical tests were performed in Prism. For multiple comparisons with 1-way ANOVA, Bonerroni posttest was used when preselected pairwise comparisons were performed, Dunnett's posttest was used when values were compared to a control set. Tukey-Kramer posttest was used when all values in the dataset were compared. A P value <0.05 was considered statistically significant. All data are mean ± SEM from independent experiments using cells from at least 4 patients.

Acknowledgements

We thank N. Cohen and L. Chandler (Philadelphia VA Medical Center) for clinical bacteria isolates and P. aeruginosa strains PAO-1 and PAO-GFP, and J. Riley (University of Pennsylvania Department of Microbiology and Human Immunology Core) for access to primary human monocytes. We thank M. Victoria (University of Pennsylvania Department of Otorhinolaryngology) for excellent technical assistance with differentiation of macrophages and molecular biology and B. Chen (University of Pennsylvania Department of Otorhinolaryngology) with assistance growing initial cultures of primary serous cells. This work was supported by grants from the Cystic Fibrosis Foundation (LEER16G0) and National Institutes of Health (R21AI137484, R01DC016309). The sponsors had no role in study design, data collection, interpretation, writing, or the decision to submit.

Author Contributions

D.B.M., M.A.K., and R.J.L. performed experiments, analyzed data, and interpreted results. M.A.K., C.C.L.T., P.P., N.D.A., and J.N.P. aided with tissue and primary cell acquisition, consenting of patients, maintenance of clinical databases and records, and intellectually contributed to interpretation of the study. R.J.L. conceived the study and wrote the paper with input and approval from all authors.

Figures

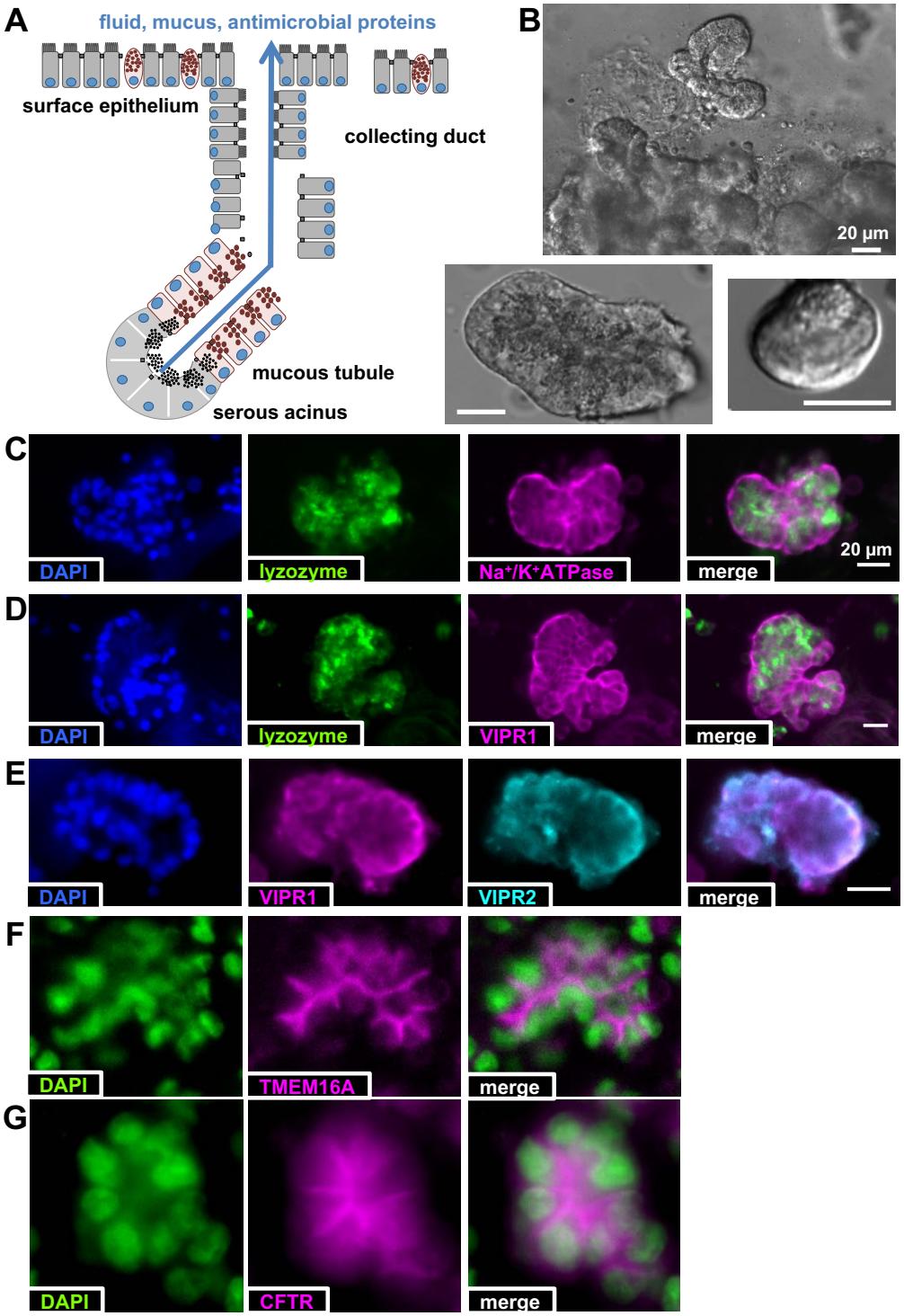

Figure 1: Isolated airway serous acinar cells. (A). Representative diagram showing serous acinar cells at the distal ends of submucosal glands, which secrete the bulk of fluid in response to agonists that utilize cAMP or Ca^{2+} as second messengers. **(B).** Primary human serous acini and acinar cells isolated from human middle turbinate samples. **(C-E).** Isolated serous acini exhibited punctate granular immunofluorescence for lysozyme as well as basolateral membrane staining for Na^+/K^+ ATPase, VIPR1, and VIPR2. **(F-G).** Apical membrane staining was observed for secretory Cl- channels TMEM16A and CFTR, as previously described. Scale bars are 20 µm.

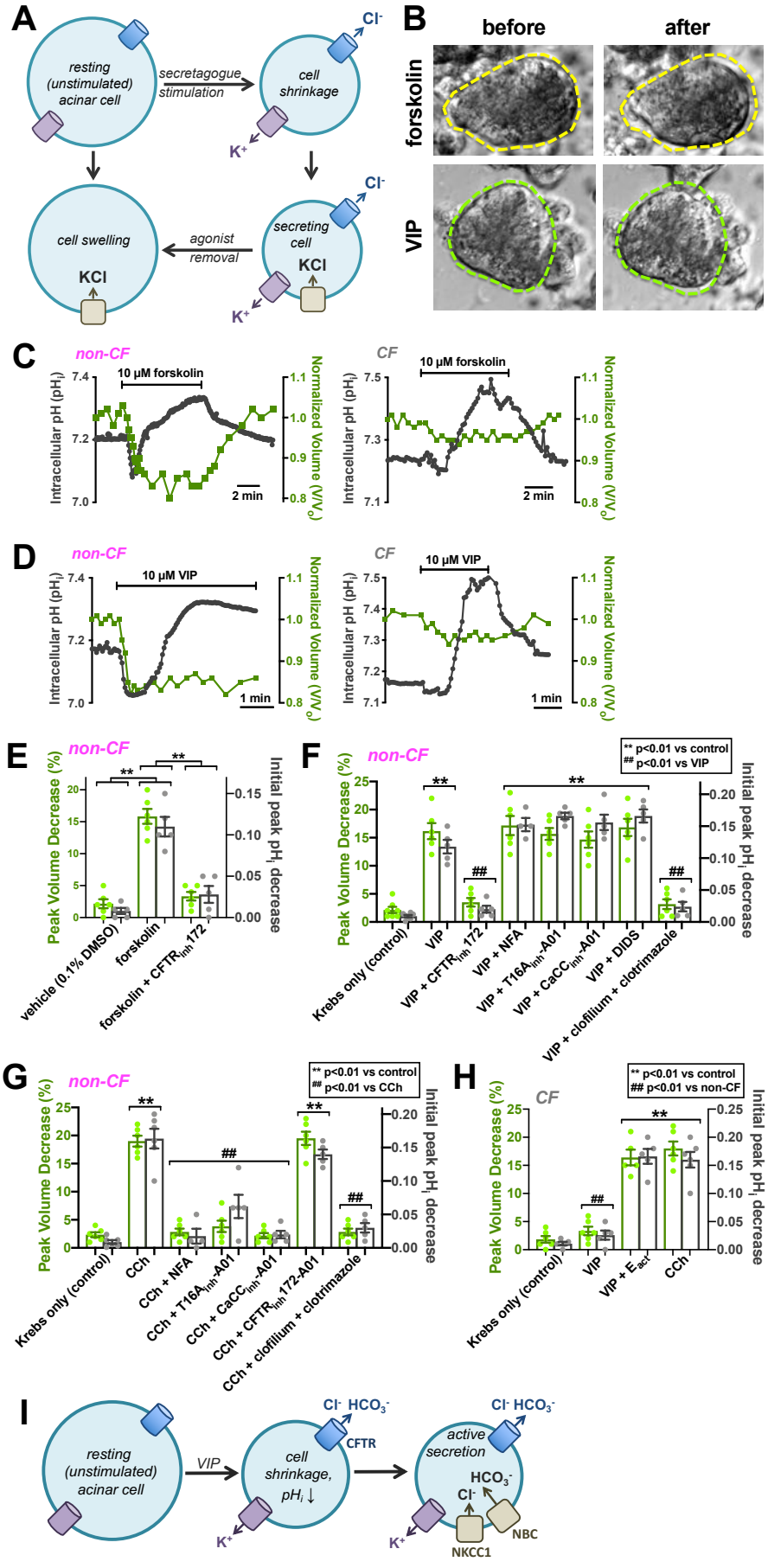

Figure 2: cAMP agonist stimulation of human nasal serous cells results in CFTR-dependent Cl^- secretion, revealed by cell shrinkage, concomitant with a CFTR-dependent decrease in pH_i. **(A)** Diagram showing use of acinar cell volume measurements to track fluid secretion, primarily driven by Cl^- secretion, which was combined with simultaneous measurement of pH_i to track HCO_3^- secretion. **(B)** Non-CF serous cells stimulated with adenylyl cyclase-activating forskolin (top) or G_s-coupled receptor agonist VIP (bottom) exhibited ~15% shrinkage reflecting the activation of fluid secretion. **(C-D)** In cells from non-CF patients, forskolin-induced (*C*) or VIP-induced (*D*) shrinkage (~15%; green) was accompanied by a transient decrease in pH_i (~0.1 unit; gray) followed by a sustained alkalinization. CF cells exhibited markedly reduced shrinkage and pH_i decrease; subsequent alkalinization was intact. **(E-H).** Bar graphs showing peak shrinkage (green) and pH_i decrease (gray) in non-CF (*E-G*) and CF (*H*) cells. Forskolin-induced shrinkage was inhibited by $CFTR_{inh}172$ (*E*), while VIP-induced shrinkage was inhibited by $CFTR_{inh}172$ and K^+ channel inhibitors clofilium and clotrimazole (*F*). Ca^{2+}-activated Cl^- channel inhibitors NFA, $T16A_{inh}$-A01, $CaCC_{inh}$-A01 or DIDS had no effect on VIP-induced shrinkage (*F*) but did block shrinkage during stimulation with a Ca^{2+}-elevating agonist carbachol (CCh). CF cells exhibited minimal responses to VIP but intact response to CCh. VIP responses were restored by TMEM16A-activator E_{act}. All experiments done at 37°C with 5% CO_2/25 mM HCO_3^-. All data in *E-H* are mean ± SEM of 5-8 individual experiments from at least 4 individual patients. Significances determined by one-way ANOVA, Bonferroni posttest. **(I)** Diagram showing activation of airway serous cell secretion by VIP, with Cl^- and HCO_3^- efflux through CFTR (apically localized in intact glands) causing a decrease in cell volume and pH_i. Influx of Cl^- though NKCC1 and influx of HCO_3^- through NBC (both basolaterally localized in intact glands) maintains the driving force for Cl^- and HCO_3^- efflux during sustained secretion.

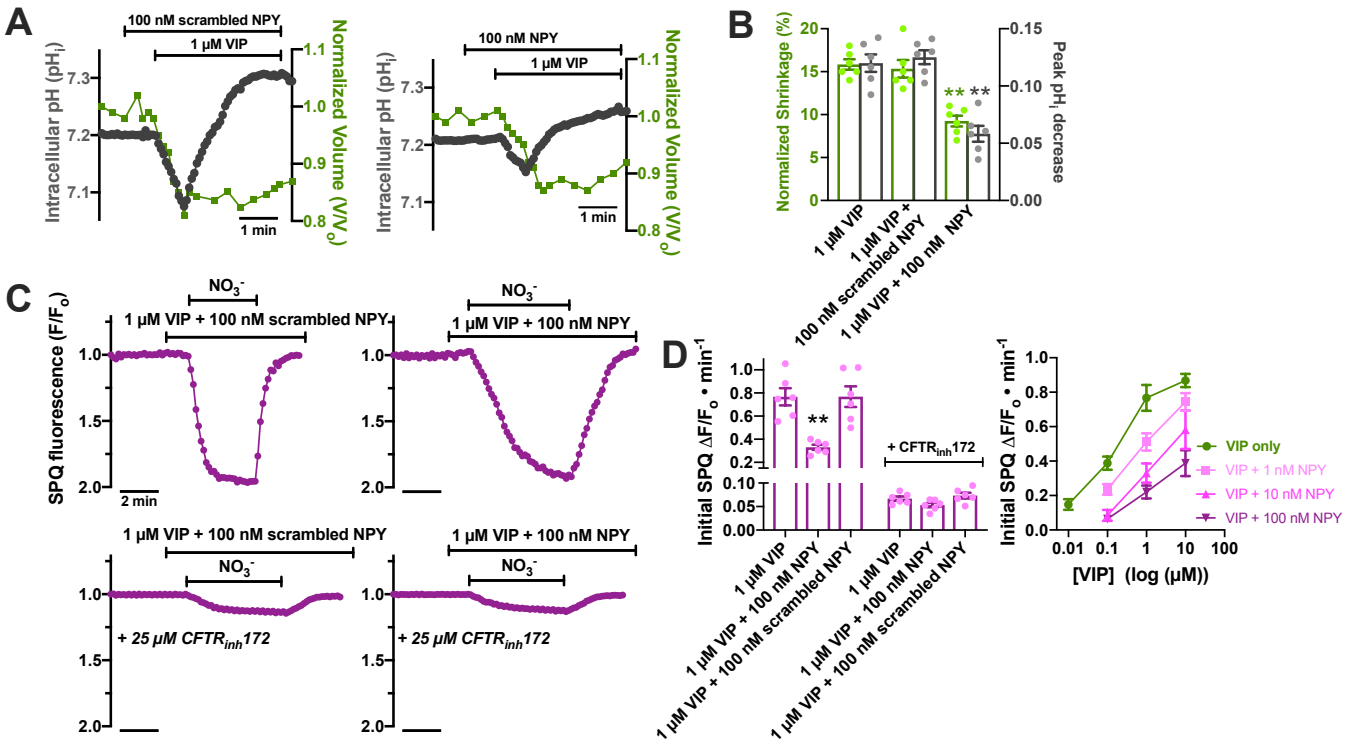

Figure 3: NPY reduces secretory response to VIP and directly reduces anion permeability though CFTR in primary nasal gland serous cells. (A). Representative traces showing cells stimulated with VIP in the presence of scrambled NPY (left) or NPY (right). **(B).** Bar graph showing mean ± SEM; cells stimulated with VIP in the presence of NPY exhibited reduced shrinkage (Cl^- secretion) and initial acidification (HCO_3^- secretion). Significance determined by 1-way ANOVA with Dunnett's posttest (VIP only as control group); ** = p<0.01 vs control. **(C).** Representative NO_3^- substitution experiments showing changes in SPQ fluorescence with substitution of Cl^-_o for $NO_3^-_o$, which causes electroneutral exchange of Cl^- for NO_3^-, a decrease in $[Cl^-]_i$, and a change SPQ fluorescence. The rate of SPQ fluorescence change reflects the relative plasma membrane anion permeability. A downward deflection equals a decrease in $[Cl^-]_i$. (D). Bar graph (left) showing initial rate of SPQ fluorescence (mean ± SEM) change after VIP stimulation, which was inhibited by NPY but not scrambled NPY. In the presence of $CFTR_{inh}172$ (10 µM), rates of SPQ fluorescence change were reduced ~10-fold and there was no effect of NPY. Right shows rates of SPQ fluorescence change over a range of VIP and NPY concentrations, showing dose dependency of VIP activation of anion permeability and NPY inhibition of anion permeability. *A* and *C* show representative traces, while *B* and *D* show data from at least 6 experiments using acinar cells from 3 patients (2 experiments per patient).

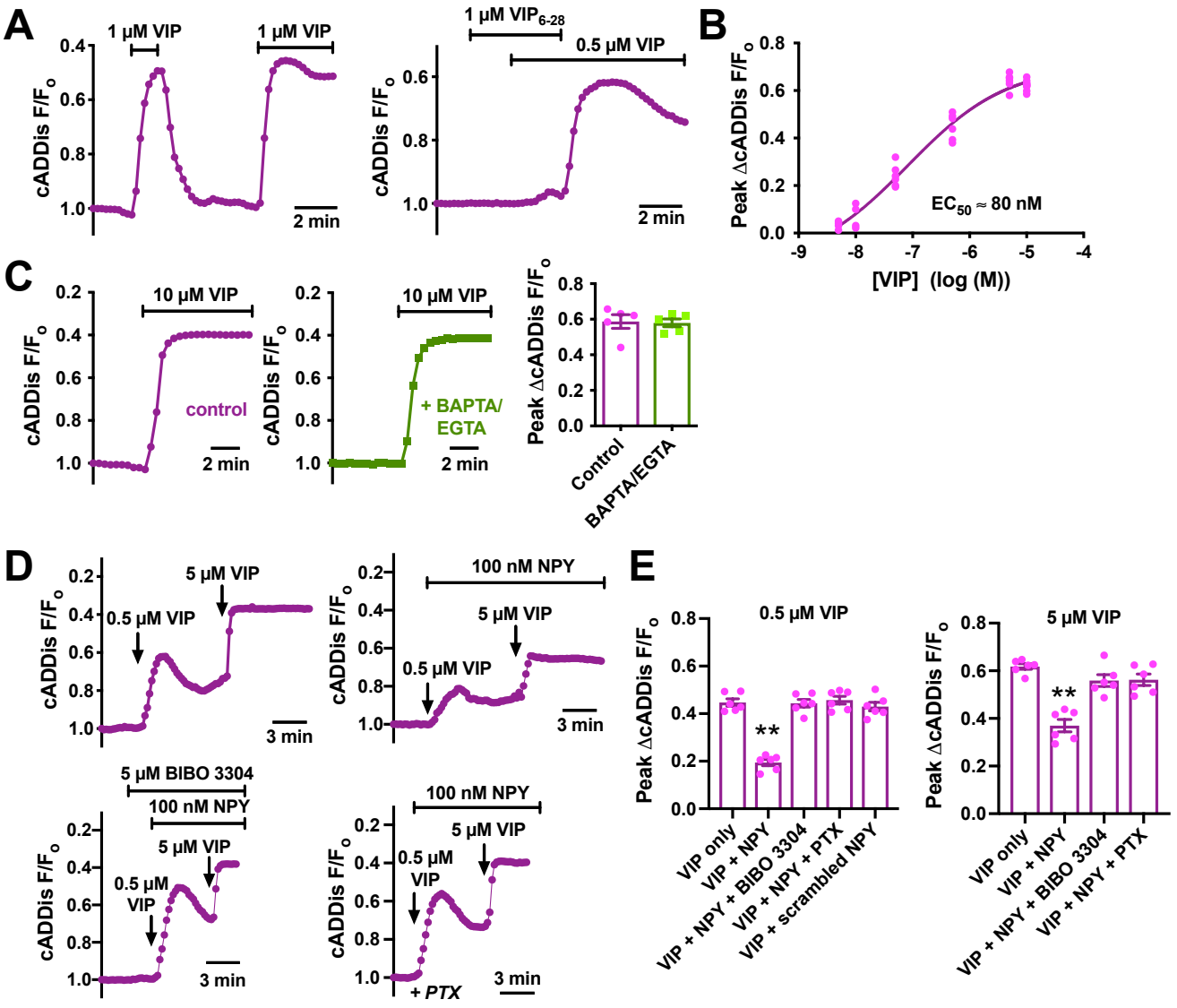

Figure 4. NPY inhibits VIP-induced cAMP increases in primary nasal gland serous cells. (A). Representative traces of cADDis fluorescence (upward deflection of trace = increase in cAMP) showing reversible VIP-activated cAMP increases blocked by VIP receptor antagonist VIP_{6-28}. **(B).** Dose response showing peak cADDis fluorescence changes with VIP. Each data point is a separate experiment; graph shows data from at least 3 serous cells from at least 3 patients (at least one per patient) for each concentration. **(C).** Representative traces (left) and bar graph (right) showing lack of inhibiton of cADDis responses by calcium chelation (10 μM BAPTA-AM loading for 30 and stimulation in solution containing no added calcium + 1 mM EGTA). Bar graph shows mean ± SEM of 5 experiments from serous cells from 2 different patients. No significant difference by Student's *t* test. **(D).** Peak cAMP responses to 0.5 μM and 5 μM VIP (top left) were inhibited by NPY (top right); NPY reduction of cAMP responses were abolished by NPY1R antagonist BIBO 3304 (bottom left) or pretreatment with pertussis toxin (PTX). **(E).** Bar graphs showing mean ± SEM of peak responses from experiments as in *D* at 2 different VIP concentrations. Shown are data points from at least 6 experiments using serous cells from at least 3 patients (at least 2 experiments per patient). Significance determined by 1-way ANOVA with Dunnett's post test (VIP only as control); ** = $p<0.01$ vs VIP only.

.

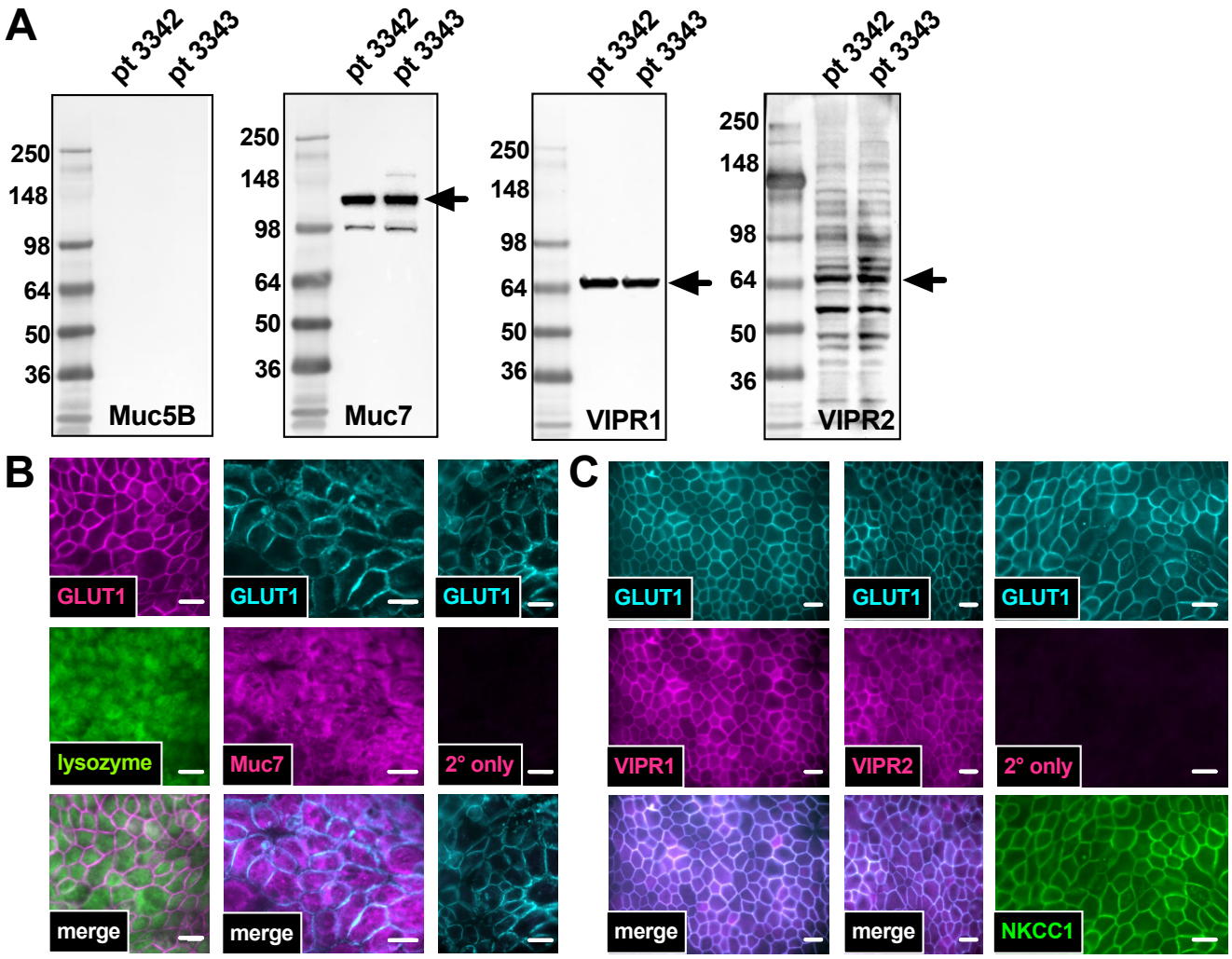

Figure 5: Expression of serous cell markers by primary nasal serous cell ALI cultures. (A). Acinar cells isolated from middle or inferior turbinate were cultured as indicated in the text. ALIs were subject to Western Blot for mucous cell marker Muc5B, serous cell marker Muc7, and VIP receptors VIPR1 and VIPR2. Results from cultures from two different patients are shown, representative of results observed from cultures at least 3 independent experiments. **(B).** Fixed cultures were immune-stained for serous cell markers lysozyme and Muc7, which showed punctate cytoplasmic staining similar to serous-like secretory granules. **(C).** Immunocytochemistry for VIPR and VIPR2 revealed basolateral staining similar to that observed with GLUT1 and NKCC1. All images in *B* and *C* are representative of results observed in cultures from at least 3 separate patients. Scale bars are 20 μm.

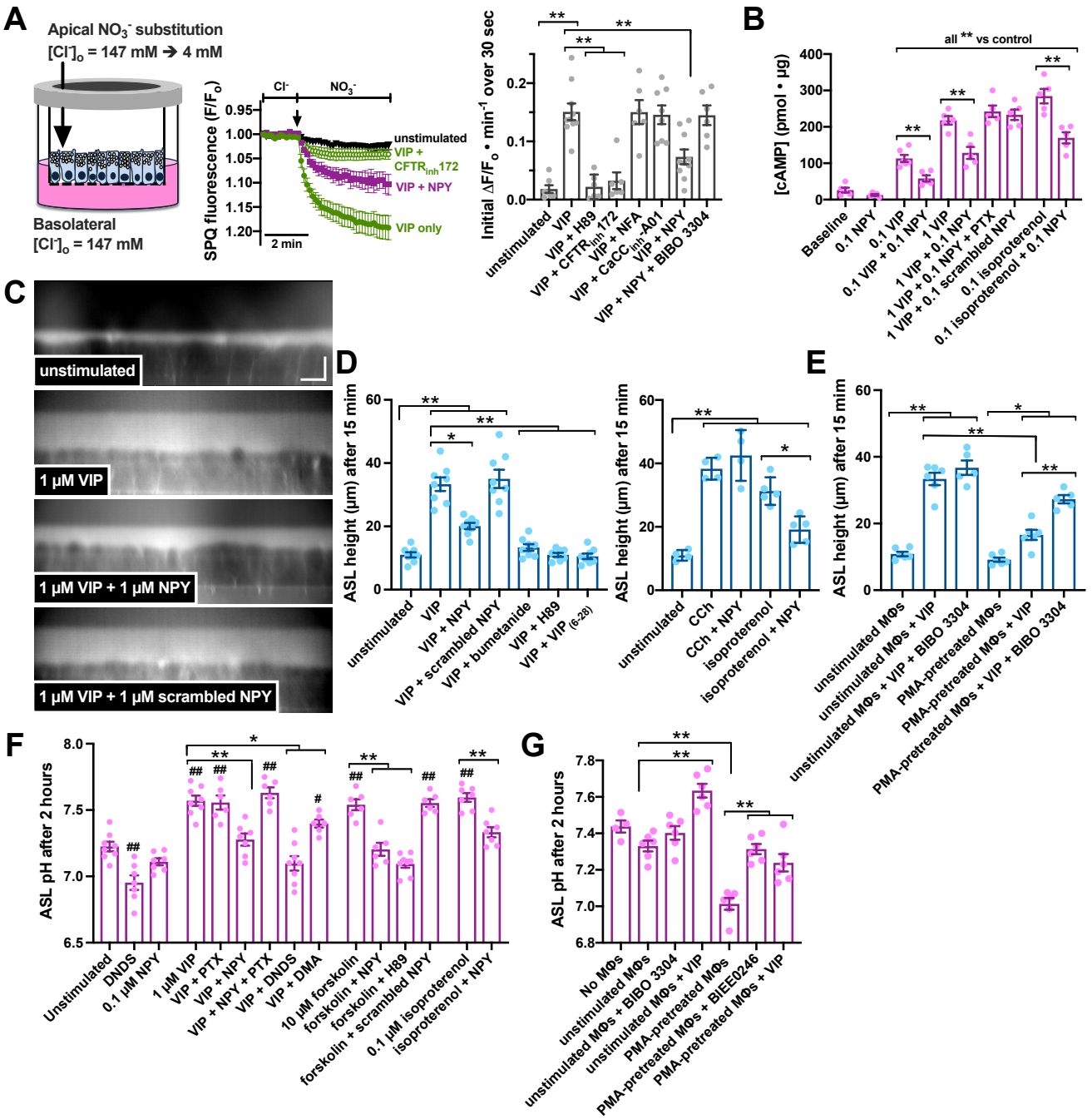

Figure 6: Modulation of fluid and HCO_3^- secretion by VIP and NPY in serous cell ALI cultures. **(A).** Apical NO_3^- substitution experiments (representative traces, left) and rates of SPQ change (bar graph right) during stimulation with VIP ± NPY in the presence or absence of indicated inhibitors. **(B).** ELISA results from steady-state cAMP measurements during stimulation with VIP or isoproterenol ± NPY or scrambled NPY. Concentrations shown are µM. Pertussis toxin (PTX) was used to demonstrate NPY effects were dependent on G_i signaling. **(C).** Representative orthogonal views of Texas red dextran-labeled ASL in primary serous cell ALIs; scale bar is 10 µm in both *x* and *z* direction. **(D).** ASL height after 15 min basolateral stimulation as indicated. **(E).** ASL height in ALIs incubated in the presence of MΦs and MΦ-conditioned media with basolateral compounds as indicated. **(F).** ASL pH measured using SNARF-1-dextran in cultures stimulated as indicated for 2 hours. Concentrations shown are µM. **(G).** ASL pH in ALIs incubated in the presence of MΦs and MΦ-conditioned media with basolateral compounds as indicated. All bar graphs show mean ± SEM of at 6 independent experiments using ALI cultures from at least 3 patients (2 cultures per patient). Significance in each bar graph determined by 1-way ANOVA with Bonferroni posttest; *= p <0.05 and ** = p <0.01 vs bracketed groups and ## and # in *F* represent p <0.05 and p <0.01, respectively vs unstimulated conditions.

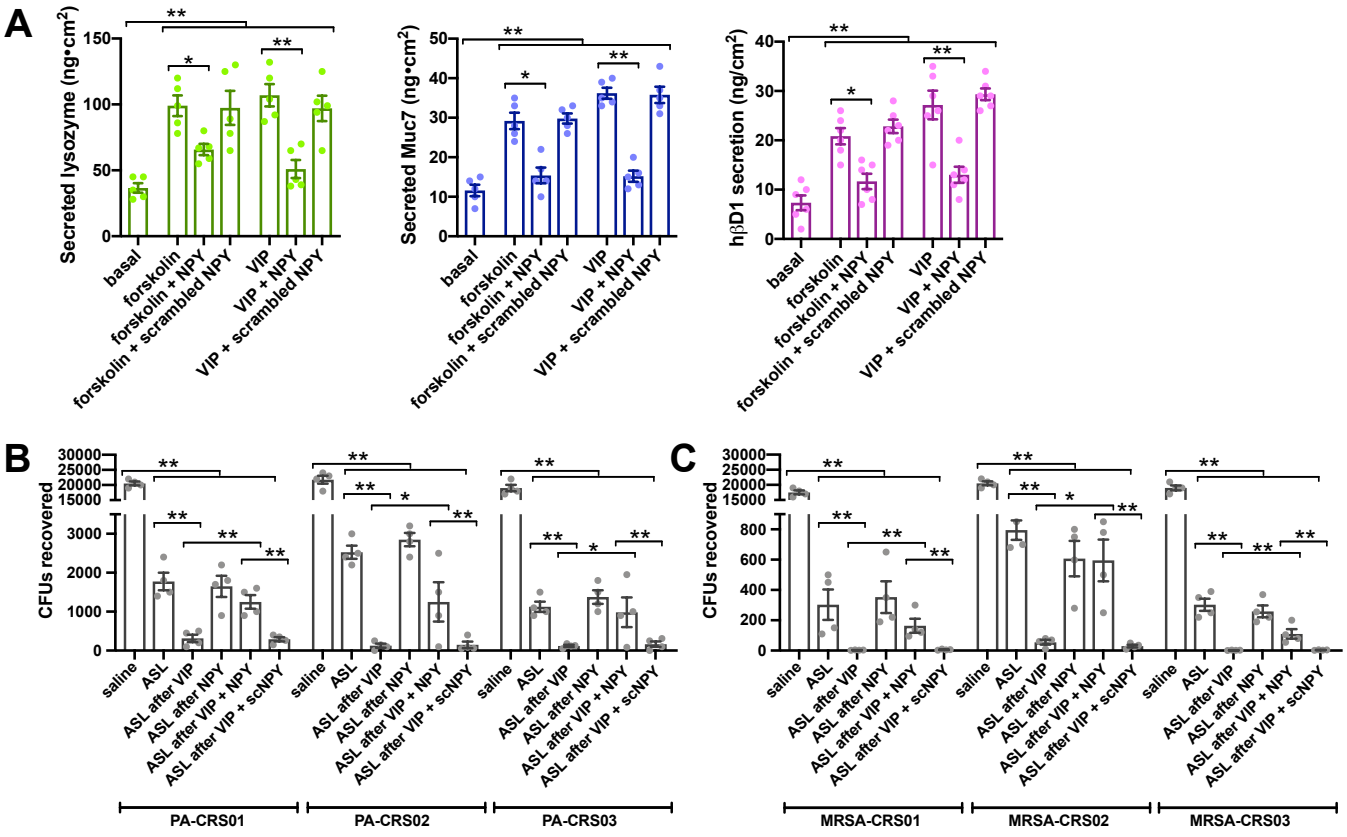

Figure 7: Antimicrobial peptide secretion and antibacterial efficacy of serous cells secretions are enhanced by VIP but reduced by NPY. (A). ALIs were stimulated basolaterally for 2 hours in the presence of forskolin (10 μM) or VIP (1 μM) ± NPY (100 nM) or scrambled NPY (100 nM) as indicated. ASL was collected by washing the apical surface with 25% saline and assayed for lysozyme, Muc7, and hβD1 by ELISA. Results shown are mean ± SEM from at least 3 ALIs from at least 3 individual patients. **(B-C).** ASL from similar experiments was mixed with strains of *P. aeruginosa* (*B*) or methicillin-resistant *S. aureus* (MRSA; *C*) isolated from CRS patients followed by incubation (37°C; 5% CO_2) and plating for CFU counting as indicated in the text. Bar graphs show mean ± SEM of at least 5 experiments using ALIs from at least 3 different patients; ** and * indicate $p<0.01$ and $p<0.05$, respectively, between bracketed groups. Significance determined by 1-way ANOVA with Bonferroni posttest.

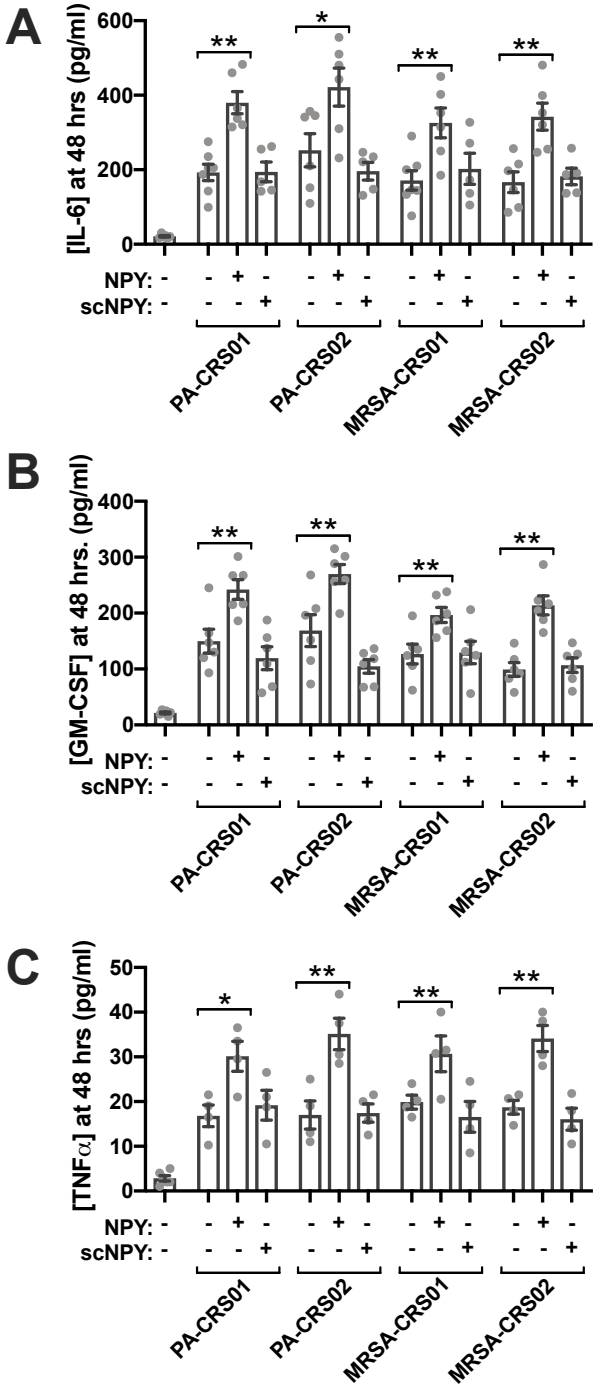

Figure 8: Serous cell cytokine secretion in response to clinical bacteria strains is increased by NPY. Primary serous cell ALIs were treated apically with heat-killed bacteria, followed by 48 hr incubation ± basolateral NPY (100 nM) or scrambled NPY (scNPY; 100 nM). Basolateral media was collected for quantification of IL-6 (*A*), GM-CSF (*B*), and TNFα (*C*). Bar graphs shown mean ± SEM of at least 5 experiments using cells grown from at least 3 different patients. Significance determined by 1-way ANOVA with Bonferroni posttest (comparing the three bars for each separate strain); ** $p<0.01$ and * $p<0.05$ between bracketed bars.

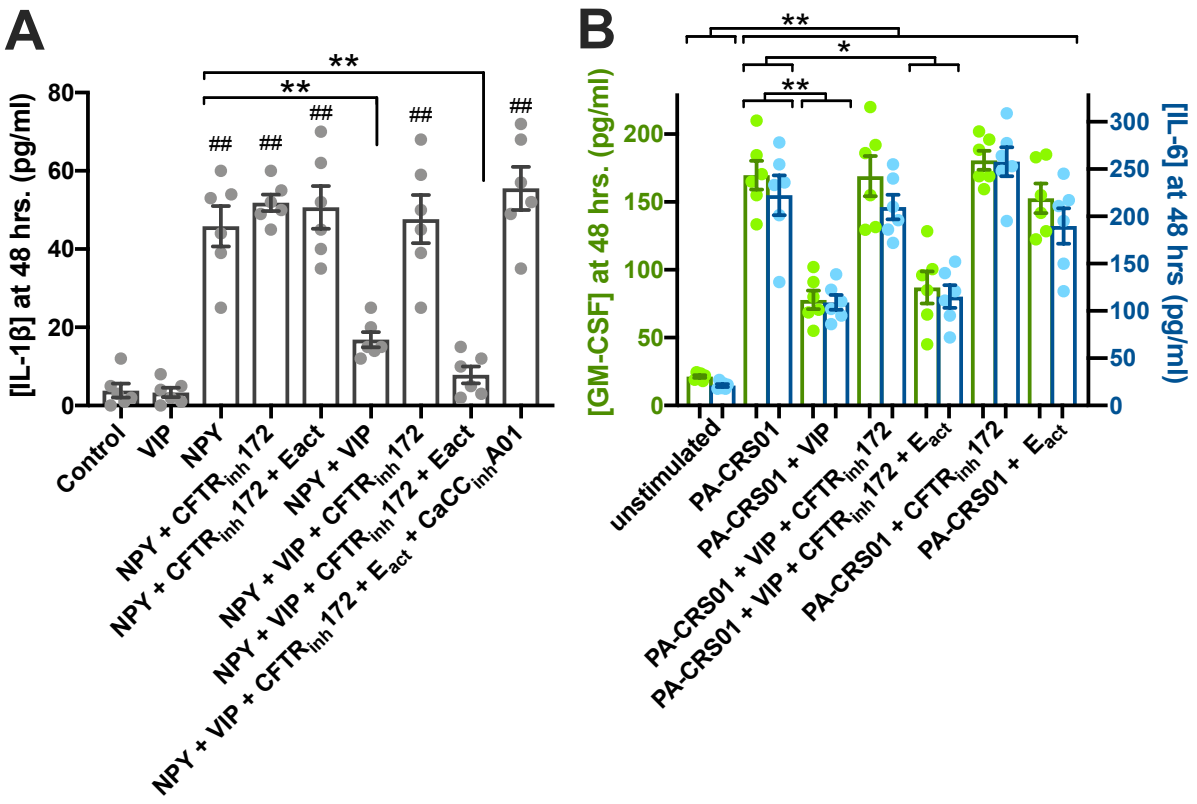

Figure 9: Anti-inflammatory effects of VIP require CFTR conductance, but can be restored by TMEM16A activation. Primary serous cell ALIs were treated basolaterally with VIP (100 μM) and/or NPY (100 nM) and treated apically with CFTR inhibitor $CFTR_{inh}172$ (15 μM), TMEM16A activator E_{act} (15 μM), and/or TMEM16A inhibitor $CaCC_{inh}$-A01 (15 μM). Basolateral media was collected after 48 hrs. and assayed for IL-1β. **(B)** Primary serous cell ALIs were treated apically with heat-killed *P. aeruginosa*, followed by 48 hrs incubation ± basolateral NPY and/or VIP as well as ± apical $CFTR_{inh}172$ and/or E_{act}. Basolateral media was collected after 48 hrs. and assayed for GM-CSF or IL-6.

References

1. Kato K, Song BH, Howe CL, and Chang EH. A Comprehensive Systematic Review of the Association Between Airway Mucins and Chronic Rhinosinusitis. *Am J Rhinol Allergy.* 2019:1945892419837042.
2. Evans CM, Kim K, Tuvim MJ, and Dickey BF. Mucus hypersecretion in asthma: causes and effects. *Curr Opin Pulm Med.* 2009;15(1):4-11.
3. Rogers DF. Physiology of airway mucus secretion and pathophysiology of hypersecretion. *Respir Care.* 2007;52(9):1134-46; discussion 46-9.
4. Rogers DF. Mucus pathophysiology in COPD: differences to asthma, and pharmacotherapy. *Monaldi Arch Chest Dis.* 2000;55(4):324-32.
5. Ballard ST, and Spadafora D. Fluid secretion by submucosal glands of the tracheobronchial airways. *Respir Physiol Neurobiol.* 2007;159(3):271-7.
6. Ballard ST, and Inglis SK. Liquid secretion properties of airway submucosal glands. *J Physiol.* 2004;556(Pt 1):1-10.
7. Widdicombe JH, and Wine JJ. Airway Gland Structure and Function. *Physiol Rev.* 2015;95(4):1241-319.
8. Engelhardt JF, Yankaskas JR, Ernst SA, Yang Y, Marino CR, Boucher RC, et al. Submucosal glands are the predominant site of CFTR expression in the human bronchus. *Nat Genet.* 1992;2(3):240-8.
9. Jacquot J, Puchelle E, Hinnrasky J, Fuchey C, Bettinger C, Spilmont C, et al. Localization of the cystic fibrosis transmembrane conductance regulator in airway secretory glands. *Eur Respir J.* 1993;6(2):169-76.
10. Lee RJ, Limberis MP, Hennessy MF, Wilson JM, and Foskett JK. Optical imaging of Ca2+-evoked fluid secretion by murine nasal submucosal gland serous acinar cells. *J Physiol.* 2007;582(Pt 3):1099-124.
11. Lee RJ, and Foskett JK. cAMP-activated Ca2+ signaling is required for CFTR-mediated serous cell fluid secretion in porcine and human airways. *J Clin Invest.* 2010;120(9):3137-48.
12. Lee RJ, and Foskett JK. Mechanisms of Ca2+-stimulated fluid secretion by porcine bronchial submucosal gland serous acinar cells. *Am J Physiol Lung Cell Mol Physiol.* 2010;298(2):22.
13. Jeffery PK, and Brain AP. Surface morphology of human airway mucosa: normal, carcinoma or cystic fibrosis. *Scanning Microsc.* 1988;2(1):553-60.
14. Ornoy A, Arnon J, Katznelson D, Granat M, Caspi B, and Chemke J. Pathological confirmation of cystic fibrosis in the fetus following prenatal diagnosis. *Am J Med Genet.* 1987;28(4):935-47.
15. Sellers ZM, Illek B, Figueira MF, Hari G, Joo NS, Sibley E, et al. Impaired PGE2-stimulated Cl- and HCO3- secretion contributes to cystic fibrosis airway disease. *PLoS One.* 2017;12(12):e0189894.
16. Joo NS, Irokawa T, Wu JV, Robbins RC, Whyte RI, and Wine JJ. Absent secretion to vasoactive intestinal peptide in cystic fibrosis airway glands. *J Biol Chem.* 2002;277(52):50710-5.
17. Joo NS, Irokawa T, Robbins RC, and Wine JJ. Hyposecretion, not hyperabsorption, is the basic defect of cystic fibrosis airway glands. *J Biol Chem.* 2006;281(11):7392-8.
18. Choi JY, Khansaheb M, Joo NS, Krouse ME, Robbins RC, Weill D, et al. Substance P stimulates human airway submucosal gland secretion mainly via a CFTR-dependent process. *J Clin Invest.* 2009;119(5):1189-200.
19. Choi JY, Joo NS, Krouse ME, Wu JV, Robbins RC, Ianowski JP, et al. Synergistic airway gland mucus secretion in response to vasoactive intestinal peptide and carbachol is lost in cystic fibrosis. *J Clin Invest.* 2007;117(10):3118-27.

20. Verkman AS, Song Y, and Thiagarajah JR. Role of airway surface liquid and submucosal glands in cystic fibrosis lung disease. *Am J Physiol Cell Physiol.* 2003;284(1):C2-15.
21. Thiagarajah JR, Song Y, Haggie PM, and Verkman AS. A small molecule CFTR inhibitor produces cystic fibrosis-like submucosal gland fluid secretions in normal airways. *FASEB J.* 2004;18(7):875-7.
22. Song Y, Salinas D, Nielson DW, and Verkman AS. Hyperacidity Of Secreted Fluid From Submucosal Glands In Early Cystic Fibrosis. *Am J Physiol Cell Physiol.* 2005.
23. Salinas D, Haggie PM, Thiagarajah JR, Song Y, Rosbe K, Finkbeiner WE, et al. Submucosal gland dysfunction as a primary defect in cystic fibrosis. *FASEB J.* 2005;19(3):431-3.
24. Jayaraman S, Joo NS, Reitz B, Wine JJ, and Verkman AS. Submucosal gland secretions in airways from cystic fibrosis patients have normal [Na(+)] and pH but elevated viscosity. *Proc Natl Acad Sci U S A.* 2001;98(14):8119-23.
25. Rogers DF. Mucus hypersecretion in chronic obstructive pulmonary disease. *Novartis Found Symp.* 2001;234:65-77; discussion -83.
26. Maestrelli P, Saetta M, Mapp CE, and Fabbri LM. Remodeling in response to infection and injury. Airway inflammation and hypersecretion of mucus in smoking subjects with chronic obstructive pulmonary disease. *Am J Respir Crit Care Med.* 2001;164(10 Pt 2):S76-80.
27. Jeffery PK. Comparative morphology of the airways in asthma and chronic obstructive pulmonary disease. *Am J Respir Crit Care Med.* 1994;150(5 Pt 2):S6-13.
28. Rogers DF. Airway mucus hypersecretion in asthma: an undervalued pathology? *Curr Opin Pharmacol.* 2004;4(3):241-50.
29. James AL, Maxwell PS, Pearce-Pinto G, Elliot JG, and Carroll NG. The relationship of reticular basement membrane thickness to airway wall remodeling in asthma. *Am J Respir Crit Care Med.* 2002;166(12 Pt 1):1590-5.
30. Groneberg DA, Eynott PR, Lim S, Oates T, Wu R, Carlstedt I, et al. Expression of respiratory mucins in fatal status asthmaticus and mild asthma. *Histopathology.* 2002;40(4):367-73.
31. Green FH, Williams DJ, James A, McPhee LJ, Mitchell I, and Mauad T. Increased myoepithelial cells of bronchial submucosal glands in fatal asthma. *Thorax.* 2010;65(1):32-8.
32. Cluroe A, Holloway L, Thomson K, Purdie G, and Beasley R. Bronchial gland duct ectasia in fatal bronchial asthma: association with interstitial emphysema. *J Clin Pathol.* 1989;42(10):1026-31.
33. Chen FH, Samson KT, Miura K, Ueno K, Odajima Y, Shougo T, et al. Airway remodeling: a comparison between fatal and nonfatal asthma. *J Asthma.* 2004;41(6):631-8.
34. Jenkins HA, Cool C, Szefler SJ, Covar R, Brugman S, Gelfand EW, et al. Histopathology of severe childhood asthma: a case series. *Chest.* 2003;124(1):32-41.
35. Woodruff PG, and Fahy JV. Airway remodeling in asthma. *Semin Respir Crit Care Med.* 2002;23(4):361-7.
36. Kunzelmann K, Schreiber R, and Hadorn HB. Bicarbonate in cystic fibrosis. *J Cyst Fibros.* 2017;16(6):653-62.
37. Gustafsson JK, Ermund A, Ambort D, Johansson ME, Nilsson HE, Thorell K, et al. Bicarbonate and functional CFTR channel are required for proper mucin secretion and link cystic fibrosis with its mucus phenotype. *J Exp Med.* 2012;209(7):1263-72.
38. Chen EY, Yang N, Quinton PM, and Chin WC. A new role for bicarbonate in mucus formation. *Am J Physiol Lung Cell Mol Physiol.* 2010;299(4):L542-9.
39. Quinton PM. Cystic fibrosis: impaired bicarbonate secretion and mucoviscidosis. *Lancet.* 2008;372(9636):415-7.

40. Joo NS, Krouse ME, Wu JV, Saenz Y, Jayaraman S, Verkman AS, et al. HCO3- transport in relation to mucus secretion from submucosal glands. *Jop.* 2001;2(4 Suppl):280-4.
41. Yang N, Garcia MA, and Quinton PM. Normal mucus formation requires cAMP-dependent HCO3- secretion and Ca2+-mediated mucin exocytosis. *J Physiol.* 2013;591(Pt 18):4581-93.
42. Kaushik KS, Stolhandske J, Shindell O, Smyth HD, and Gordon VD. Tobramycin and bicarbonate synergise to kill planktonic Pseudomonas aeruginosa, but antagonise to promote biofilm survival. *NPJ Biofilms Microbiomes.* 2016;2:16006.
43. Massip-Copiz MM, and Santa-Coloma TA. Extracellular pH and lung infections in cystic fibrosis. *Eur J Cell Biol.* 2018.
44. Newbrun E, Hoover CI, and Ryder MI. Bactericidal action of bicarbonate ion on selected periodontal pathogenic microorganisms. *J Periodontol.* 1984;55(11):658-67.
45. Dorschner RA, Lopez-Garcia B, Peschel A, Kraus D, Morikawa K, Nizet V, et al. The mammalian ionic environment dictates microbial susceptibility to antimicrobial defense peptides. *FASEB J.* 2006;20(1):35-42.
46. Lee RJ, and Foskett JK. Ca2+ signaling and fluid secretion by secretory cells of the airway epithelium. *Cell Calcium.* 2014;55(6):325-36.
47. Lee RJ, Harlow JM, Limberis MP, Wilson JM, and Foskett JK. HCO3(-) secretion by murine nasal submucosal gland serous acinar cells during Ca2+-stimulated fluid secretion. *J Gen Physiol.* 2008;132(1):161-83.
48. Lee RJ, and Foskett JK. Why mouse airway submucosal gland serous cells do not secrete fluid in response to cAMP stimulation. *J Biol Chem.* 2012;287(45):38316-26.
49. Atanasova KR, and Reznikov LR. Neuropeptides in asthma, chronic obstructive pulmonary disease and cystic fibrosis. *Respir Res.* 2018;19(1):149.
50. Baraniuk JN, and Kaliner MA. Neuropeptides and nasal secretion. *J Allergy Clin Immunol.* 1990;86(4 Pt 2):620-7.
51. Baraniuk JN, Lundgren JD, Okayama M, Mullol J, Merida M, Shelhamer JH, et al. Vasoactive intestinal peptide in human nasal mucosa. *J Clin Invest.* 1990;86(3):825-31.
52. Dey RD, Shannon WA, Jr., and Said SI. Localization of VIP-immunoreactive nerves in airways and pulmonary vessels of dogs, cat, and human subjects. *Cell Tissue Res.* 1981;220(2):231-8.
53. Mendonca JC, and Dolci JE. Neuropeptide immunofluorescence in human nasal mucosa: assessment of the technique for vasoactive intestinal peptide (VIP). *Braz J Otorhinolaryngol.* 2005;71(2):123-31.
54. Uddman R, and Sundler F. Neuropeptides in the airways: a review. *Am Rev Respir Dis.* 1987;136(6 Pt 2):S3-8.
55. Uddman R, Alumets J, Densert O, Hakanson R, and Sundler F. Occurrence and distribution of VIP nerves in the nasal mucosa and tracheobronchial wall. *Acta Otolaryngol.* 1978;86(5-6):443-8.
56. Sheppard MN, Polak JM, Allen JM, and Bloom SR. Neuropeptide tyrosine (NPY): a newly discovered peptide is present in the mammalian respiratory tract. *Thorax.* 1984;39(5):326-30.
57. Chanez P, Springall D, Vignola AM, Moradoghi-Hattvani A, Polak JM, Godard P, et al. Bronchial mucosal immunoreactivity of sensory neuropeptides in severe airway diseases. *Am J Respir Crit Care Med.* 1998;158(3):985-90.
58. Tanaka Y, Yoshida Y, and Hirano M. Precise localization of VIP-, NPY-, and TH-immunoreactivities of cat laryngeal glands. *Brain Res Bull.* 1995;36(3):219-24.
59. Bowden JJ, and Gibbins IL. Vasoactive intestinal peptide and neuropeptide Y coexist in non-noradrenergic sympathetic neurons to guinea pig trachea. *J Auton Nerv Syst.* 1992;38(1):1-19.

60. Luts A, Uddman R, Alm P, Basterra J, and Sundler F. Peptide-containing nerve fibers in human airways: distribution and coexistence pattern. *Int Arch Allergy Immunol.* 1993;101(1):52-60.
61. Uddman R, Sundler F, and Emson P. Occurrence and distribution of neuropeptide-Y-immunoreactive nerves in the respiratory tract and middle ear. *Cell Tissue Res.* 1984;237(2):321-7.
62. Schwarz H, Villiger PM, von Kempis J, and Lotz M. Neuropeptide Y is an inducible gene in the human immune system. *J Neuroimmunol.* 1994;51(1):53-61.
63. Fujiwara S, Hoshizaki M, Ichida Y, Lex D, Kuroda E, Ishii KJ, et al. Pulmonary phagocyte-derived NPY controls the pathology of severe influenza virus infection. *Nat Microbiol.* 2019;4(2):258-68.
64. Singer K, Morris DL, Oatmen KE, Wang T, DelProposto J, Mergian T, et al. Neuropeptide Y is produced by adipose tissue macrophages and regulates obesity-induced inflammation. *PLoS One.* 2013;8(3):e57929.
65. Li S, Koziol-White C, Jude J, Jiang M, Zhao H, Cao G, et al. Epithelium-generated neuropeptide Y induces smooth muscle contraction to promote airway hyperresponsiveness. *J Clin Invest.* 2016;126(5):1978-82.
66. Makinde TO, Steininger R, and Agrawal DK. NPY and NPY receptors in airway structural and inflammatory cells in allergic asthma. *Exp Mol Pathol.* 2013;94(1):45-50.
67. Groneberg DA, Folkerts G, Peiser C, Chung KF, and Fischer A. Neuropeptide Y (NPY). *Pulm Pharmacol Ther.* 2004;17(4):173-80.
68. Lu Y, Andiappan AK, Lee B, Ho R, Lim TK, Kuan WS, et al. Neuropeptide Y associated with asthma in young adults. *Neuropeptides.* 2016;59:117-21.
69. Lu Y, Van Bever HP, Lim TK, Kuan WS, Goh DY, Mahadevan M, et al. Obesity, asthma prevalence and IL-4: Roles of inflammatory cytokines, adiponectin and neuropeptide Y. *Pediatr Allergy Immunol.* 2015;26(6):530-6.
70. Lu Y, Ho R, Lim TK, Kuan WS, Goh DY, Mahadevan M, et al. Neuropeptide Y may mediate psychological stress and enhance TH2 inflammatory response in asthma. *J Allergy Clin Immunol.* 2015;135(4):1061-3 e4.
71. Heppt W, Dinh QT, Cryer A, Zweng M, Noga O, Peiser C, et al. Phenotypic alteration of neuropeptide-containing nerve fibres in seasonal intermittent allergic rhinitis. *Clin Exp Allergy.* 2004;34(7):1105-10.
72. Fischer A, Wussow A, Cryer A, Schmeck B, Noga O, Zweng M, et al. Neuronal plasticity in persistent perennial allergic rhinitis. *J Occup Environ Med.* 2005;47(1):20-5.
73. Groneberg DA, Heppt W, Cryer A, Wussow A, Peiser C, Zweng M, et al. Toxic rhinitis-induced changes of human nasal mucosa innervation. *Toxicol Pathol.* 2003;31(3):326-31.
74. Fang SY, Shen CL, and Ohyama M. Presence of neuropeptides in human nasal polyps. *Acta Otolaryngol.* 1994;114(3):324-8.
75. Macia L, Rao PT, Wheway J, Sierro F, Mackay F, and Herzog H. Y1 signalling has a critical role in allergic airway inflammation. *Immunol Cell Biol.* 2011;89(8):882-8.
76. Prod'homme T, Weber MS, Steinman L, and Zamvil SS. A neuropeptide in immune-mediated inflammation, Y? *Trends Immunol.* 2006;27(4):164-7.
77. Buttari B, Profumo E, Domenici G, Tagliani A, Ippoliti F, Bonini S, et al. Neuropeptide Y induces potent migration of human immature dendritic cells and promotes a Th2 polarization. *FASEB J.* 2014;28(7):3038-49.
78. Wine JJ. Parasympathetic control of airway submucosal glands: central reflexes and the airway intrinsic nervous system. *Auton Neurosci.* 2007;133(1):35-54.

79. Merten MD, and Figarella C. Neuropeptide Y and norepinephrine cooperatively inhibit human tracheal gland cell secretion. *Am J Physiol.* 1994;266(5 Pt 1):L513-8.
80. Webber SE. The effects of peptide histidine isoleucine and neuropeptide Y on mucus volume output from the ferret trachea. *Br J Pharmacol.* 1988;95(1):49-54.
81. Harada Y, Okubo M, Yaga K, Kaneko T, and Kaku K. Neuropeptide Y inhibits beta-adrenergic agonist- and vasoactive intestinal peptide-induced cyclic AMP accumulation in rat pinealocytes through pertussis toxin-sensitive G protein. *J Neurochem.* 1992;59(6):2178-83.
82. Huang SC, and Tsai MF. Receptors for peptide YY and neuropeptide Y on guinea pig pancreatic acini. *Peptides.* 1994;15(3):405-10.
83. Silva P, Epstein FH, Karnaky KJ, Jr., Reichlin S, and Forrest JN, Jr. Neuropeptide Y inhibits chloride secretion in the shark rectal gland. *Am J Physiol.* 1993;265(2 Pt 2):R439-46.
84. Grandt D, Siewert J, Sieburg B, al Tai O, Schimiczek M, Goebell H, et al. Peptide YY inhibits exocrine pancreatic secretion in isolated perfused rat pancreas by Y1 receptors. *Pancreas.* 1995;10(2):180-6.
85. Chandrasekharan B, Nezami BG, and Srinivasan S. Emerging neuropeptide targets in inflammation: NPY and VIP. *Am J Physiol Gastrointest Liver Physiol.* 2013;304(11):G949-57.
86. Foskett JK, and Melvin JE. Activation of salivary secretion: coupling of cell volume and [Ca2+]i in single cells. *Science.* 1989;244(4912):1582-5.
87. Foskett JK. In: Grinstein S, and Foskett, J. K. ed. *Noninvasive Techniques in Cell Biology*. New York: Wiley-Liss, Inc.; 1990:237-72.
88. Huang J, Kim D, Shan J, Abu-Arish A, Luo Y, and Hanrahan JW. Most bicarbonate secretion by Calu-3 cells is mediated by CFTR and independent of pendrin. *Physiol Rep.* 2018;6(5).
89. Kim D, Kim J, Burghardt B, Best L, and Steward MC. Role of anion exchangers in Cl- and HCO3- secretion by the human airway epithelial cell line Calu-3. *Am J Physiol Cell Physiol.* 2014;307(2):C208-19.
90. Garnett JP, Hickman E, Burrows R, Hegyi P, Tiszlavicz L, Cuthbert AW, et al. Novel role for pendrin in orchestrating bicarbonate secretion in cystic fibrosis transmembrane conductance regulator (CFTR)-expressing airway serous cells. *J Biol Chem.* 2011;286(47):41069-82.
91. Garnett JP, Hickman E, Tunkamnerdthai O, Cuthbert AW, and Gray MA. Protein phosphatase 1 coordinates CFTR-dependent airway epithelial HCO3- secretion by reciprocal regulation of apical and basolateral membrane Cl(-)-HCO3- exchangers. *Br J Pharmacol.* 2013;168(8):1946-60.
92. McMahon DB, Workman AD, Kohanski MA, Carey RM, Freund JR, Hariri BM, et al. Protease-activated receptor 2 activates airway apical membrane chloride permeability and increases ciliary beating. *FASEB J.* 2018;32(1):155-67.
93. Verkman AS, Sellers MC, Chao AC, Leung T, and Ketcham R. Synthesis and characterization of improved chloride-sensitive fluorescent indicators for biological applications. *Anal Biochem.* 1989;178(2):355-61.
94. Tewson PH, Martinka S, Shaner NC, Hughes TE, and Quinn AM. New DAG and cAMP Sensors Optimized for Live-Cell Assays in Automated Laboratories. *J Biomol Screen.* 2016;21(3):298-305.
95. Kunzelmann K, and Mehta A. CFTR: a hub for kinases and crosstalk of cAMP and Ca2+. *FEBS J.* 2013;280(18):4417-29.
96. Finkbeiner WE, Zlock LT, Mehdi I, and Widdicombe JH. Cultures of human tracheal gland cells of mucous or serous phenotype. *In Vitro Cell Dev Biol Anim.* 2010;46(5):450-6.
97. Finkbeiner WE, Zlock LT, Morikawa M, Lao AY, Dasari V, and Widdicombe JH. Cystic fibrosis and the relationship between mucin and chloride secretion by cultures of human airway gland mucous cells. *Am J Physiol Lung Cell Mol Physiol.* 2011;301(4):L402-14.

98. Widdicombe JH, Borthwell RM, Hajighasemi-Ossareh M, Lachowicz-Scroggins ME, Finkbeiner WE, Stevens JE, et al. Chloride secretion by cultures of pig tracheal gland cells. *Am J Physiol Lung Cell Mol Physiol.* 2012;302(10):L1098-106.
99. Sharma P, Dudus L, Nielsen PA, Clausen H, Yankaskas JR, Hollingsworth MA, et al. MUC5B and MUC7 are differentially expressed in mucous and serous cells of submucosal glands in human bronchial airways. *Am J Respir Cell Mol Biol.* 1998;19(1):30-7.
100. Dubin RF, Robinson SK, and Widdicombe JH. Secretion of lactoferrin and lysozyme by cultures of human airway epithelium. *Am J Physiol Lung Cell Mol Physiol.* 2004;286(4):L750-5.
101. Dajani R, Zhang Y, Taft PJ, Travis SM, Starner TD, Olsen A, et al. Lysozyme Secretion by Submucosal Glands Protects the Airway From Bacterial Infection. *Am J Respir Cell Mol Biol.* 2005.
102. Worthington EN, and Tarran R. Methods for ASL measurements and mucus transport rates in cell cultures. *Methods Mol Biol.* 2011;742:77-92.
103. Kreda SM, Seminario-Vidal L, van Heusden CA, O'Neal W, Jones L, Boucher RC, et al. Receptor-promoted exocytosis of airway epithelial mucin granules containing a spectrum of adenine nucleotides. *J Physiol.* 2010;588(Pt 12):2255-67.
104. Kreda SM, Okada SF, van Heusden CA, O'Neal W, Gabriel S, Abdullah L, et al. Coordinated release of nucleotides and mucin from human airway epithelial Calu-3 cells. *J Physiol.* 2007;584(Pt 1):245-59.
105. Dobay O, Laub K, Stercz B, Keri A, Balazs B, Tothpal A, et al. Bicarbonate Inhibits Bacterial Growth and Biofilm Formation of Prevalent Cystic Fibrosis Pathogens. *Front Microbiol.* 2018;9:2245.
106. Dimitrijevic M, and Stanojevic S. The intriguing mission of neuropeptide Y in the immune system. *Amino Acids.* 2013;45(1):41-53.
107. Wheway J, Herzog H, and Mackay F. NPY and receptors in immune and inflammatory diseases. *Curr Top Med Chem.* 2007;7(17):1743-52.
108. Ganea D, Hooper KM, and Kong W. The neuropeptide vasoactive intestinal peptide: direct effects on immune cells and involvement in inflammatory and autoimmune diseases. *Acta Physiol (Oxf).* 2015;213(2):442-52.
109. Delgado M, and Ganea D. Vasoactive intestinal peptide: a neuropeptide with pleiotropic immune functions. *Amino Acids.* 2013;45(1):25-39.
110. Hauk V, Calafat M, Larocca L, Fraccaroli L, Grasso E, Ramhorst R, et al. Vasoactive intestinal peptide/vasoactive intestinal peptide receptor relative expression in salivary glands as one endogenous modulator of acinar cell apoptosis in a murine model of Sjogren's syndrome. *Clin Exp Immunol.* 2011;166(3):309-16.
111. Vanesa H, Mario C, Esteban G, Laura F, Daniel P, Rosanna R, et al. Neuroimmune aspects of Sjogren's syndrome: role of VIP/VPAC system in immune and salivary gland epithelial cell function. *Curr Pharm Des.* 2014;20(29):4760-5.
112. Calafat M, Larocca L, Roca V, Hauk V, Pregi N, Nesse A, et al. Vasoactive intestinal peptide inhibits TNF-alpha-induced apoptotic events in acinar cells from nonobese diabetic mice submandibular glands. *Arthritis Res Ther.* 2009;11(2):R53.
113. Li C, Zhu F, Wu B, and Wang Y. Vasoactive Intestinal Peptide Protects Salivary Glands against Structural Injury and Secretory Dysfunction via IL-17A and AQP5 Regulation in a Model of Sjogren Syndrome. *Neuroimmunomodulation.* 2017;24(6):300-9.
114. Dios ID. Inflammatory role of the acinar cells during acute pancreatitis. *World J Gastrointest Pharmacol Ther.* 2010;1(1):15-20.

115. Yamakawa M, Weinstein R, Tsuji T, McBride J, Wong DT, and Login GR. Age-related alterations in IL-1beta, TNF-alpha, and IL-6 concentrations in parotid acinar cells from BALB/c and non-obese diabetic mice. *J Histochem Cytochem.* 2000;48(8):1033-42.
116. Tanda N, Ohyama H, Yamakawa M, Ericsson M, Tsuji T, McBride J, et al. IL-1 beta and IL-6 in mouse parotid acinar cells: characterization of synthesis, storage, and release. *Am J Physiol.* 1998;274(1 Pt 1):G147-56.
117. Kempuraj D, Twait EC, Williard DE, Yuan Z, Meyerholz DK, and Samuel I. The novel cytokine interleukin-33 activates acinar cell proinflammatory pathways and induces acute pancreatic inflammation in mice. *PLoS One.* 2013;8(2):e56866.
118. Zhu L, Lee PK, Lee WM, Zhao Y, Yu D, and Chen Y. Rhinovirus-induced major airway mucin production involves a novel TLR3-EGFR-dependent pathway. *Am J Respir Cell Mol Biol.* 2009;40(5):610-9.
119. Yamaya M, Sekizawa K, Suzuki T, Yamada N, Furukawa M, Ishizuka S, et al. Infection of human respiratory submucosal glands with rhinovirus: effects on cytokine and ICAM-1 production. *Am J Physiol.* 1999;277(2):L362-71.
120. Murakami K, Tamada T, Nara M, Muramatsu S, Kikuchi T, Kanehira M, et al. Toll-like receptor 4 potentiates Ca2+-dependent secretion of electrolytes from swine tracheal glands. *Am J Respir Cell Mol Biol.* 2011;45(5):1101-10.
121. Hauber HP, Tulic MK, Tsicopoulos A, Wallaert B, Olivenstein R, Daigneault P, et al. Toll-like receptors 4 and 2 expression in the bronchial mucosa of patients with cystic fibrosis. *Can Respir J.* 2005;12(1):13-8.
122. White SR, Martin LD, Stern R, Laxman B, and Marroquin BA. Expression of IL-4/IL-13 receptors in differentiating human airway epithelial cells. *Am J Physiol Lung Cell Mol Physiol.* 2010;299(5):L681-93.
123. Herbert C, Do K, Chiu V, Garthwaite L, Chen Y, Young PM, et al. Allergic environment enhances airway epithelial pro-inflammatory responses to rhinovirus infection. *Clin Sci (Lond).* 2017;131(6):499-509.
124. Veit G, Bossard F, Goepp J, Verkman AS, Galietta LJ, Hanrahan JW, et al. Proinflammatory cytokine secretion is suppressed by TMEM16A or CFTR channel activity in human cystic fibrosis bronchial epithelia. *Mol Biol Cell.* 2012;23(21):4188-202.
125. Schnur A, Hegyi P, Rousseau S, Lukacs GL, and Veit G. Epithelial Anion Transport as Modulator of Chemokine Signaling. *Mediators Inflamm.* 2016;2016:7596531.
126. Zhang YL, Chen PX, Guan WJ, Guo HM, Qiu ZE, Xu JW, et al. Increased intracellular Cl(-) concentration promotes ongoing inflammation in airway epithelium. *Mucosal Immunol.* 2018;11(4):1149-57.
127. Gentzsch M, and Mall MA. Ion Channel Modulators in Cystic Fibrosis. *Chest.* 2018;154(2):383-93.
128. Li H, Salomon JJ, Sheppard DN, Mall MA, and Galietta LJ. Bypassing CFTR dysfunction in cystic fibrosis with alternative pathways for anion transport. *Curr Opin Pharmacol.* 2017;34:91-7.
129. Lee RJ, Workman AD, Carey RM, Chen B, Rosen PL, Doghramji L, et al. Fungal Aflatoxins Reduce Respiratory Mucosal Ciliary Function. *Sci Rep.* 2016;6:33221.
130. Wong LB, Park CL, and Yeates DB. Neuropeptide Y inhibits ciliary beat frequency in human ciliated cells via nPKC, independently of PKA. *Am J Physiol.* 1998;275(2 Pt 1):C440-8.
131. Cervin A, Lindberg S, and Mercke U. The effect of neuropeptide Y on mucociliary activity in the rabbit maxillary sinus. *Acta Otolaryngol.* 1991;111(5):960-6.
132. Cervin A. Neuropeptide Y 16-36 inhibits mucociliary activity but does not affect blood flow in the rabbit maxillary sinus in vivo. *Regul Pept.* 1992;39(2-3):237-46.

133. Reid L. Measurement of the bronchial mucous gland layer: a diagnostic yardstick in chronic bronchitis. *Thorax.* 1960;15:132-41.
134. Meyrick B, and Reid L. Ultrastructure of cells in the human bronchial submucosal glands. *J Anat.* 1970;107(Pt 2):281-99.
135. Meyrick B, Sturgess JM, and Reid L. A reconstruction of the duct system and secretory tubules of the human bronchial submucosal gland. *Thorax.* 1969;24(6):729-36.
136. Schleimer RP, and Berdnikovs S. Etiology of epithelial barrier dysfunction in patients with type 2 inflammatory diseases. *J Allergy Clin Immunol.* 2017;139(6):1752-61.
137. Pothoven KL, and Schleimer RP. The barrier hypothesis and Oncostatin M: Restoration of epithelial barrier function as a novel therapeutic strategy for the treatment of type 2 inflammatory disease. *Tissue Barriers.* 2017;5(3):e1341367.
138. Heijink IH, Nawijn MC, and Hackett TL. Airway epithelial barrier function regulates the pathogenesis of allergic asthma. *Clin Exp Allergy.* 2014;44(5):620-30.
139. Kawaguchi M, Kokubu F, Odaka M, Watanabe S, Suzuki S, Ieki K, et al. Induction of granulocyte-macrophage colony-stimulating factor by a new cytokine, ML-1 (IL-17F), via Raf I-MEK-ERK pathway. *J Allergy Clin Immunol.* 2004;114(2):444-50.
140. Reibman J, Talbot AT, Hsu Y, Ou G, Jover J, Nilsen D, et al. Regulation of expression of granulocyte-macrophage colony-stimulating factor in human bronchial epithelial cells: roles of protein kinase C and mitogen-activated protein kinases. *J Immunol.* 2000;165(3):1618-25.
141. Roan F, Obata-Ninomiya K, and Ziegler SF. Epithelial cell-derived cytokines: more than just signaling the alarm. *J Clin Invest.* 2019;129(4):1441-51.
142. Yang Y, Bin W, Aksoy MO, and Kelsen SG. Regulation of interleukin-1beta and interleukin-1beta inhibitor release by human airway epithelial cells. *Eur Respir J.* 2004;24(3):360-6.
143. Laan M, Prause O, Miyamoto M, Sjostrand M, Hytonen AM, Kaneko T, et al. A role of GM-CSF in the accumulation of neutrophils in the airways caused by IL-17 and TNF-alpha. *Eur Respir J.* 2003;21(3):387-93.
144. Furukawa E, Ohrui T, Yamaya M, Suzuki T, Nakasato H, Sasaki T, et al. Human airway submucosal glands augment eosinophil chemotaxis during rhinovirus infection. *Clin Exp Allergy.* 2004;34(5):704-11.
145. Ritz SA, Cundall MJ, Gajewska BU, Swirski FK, Wiley RE, Alvarez D, et al. The lung cytokine microenvironment influences molecular events in the lymph nodes during Th1 and Th2 respiratory mucosal sensitization to antigen in vivo. *Clin Exp Immunol.* 2004;138(2):213-20.
146. Ritz SA, Cundall MJ, Gajewska BU, Alvarez D, Gutierrez-Ramos JC, Coyle AJ, et al. Granulocyte macrophage colony-stimulating factor-driven respiratory mucosal sensitization induces Th2 differentiation and function independently of interleukin-4. *Am J Respir Cell Mol Biol.* 2002;27(4):428-35.
147. Nakamura Y, Azuma M, Okano Y, Sano T, Takahashi T, Ohmoto Y, et al. Upregulatory effects of interleukin-4 and interleukin-13 but not interleukin-10 on granulocyte/macrophage colony-stimulating factor production by human bronchial epithelial cells. *Am J Respir Cell Mol Biol.* 1996;15(5):680-7.
148. Levy H, Murphy A, Zou F, Gerard C, Klanderman B, Schuemann B, et al. IL1B polymorphisms modulate cystic fibrosis lung disease. *Pediatr Pulmonol.* 2009;44(6):580-93.
149. Erbek SS, Yurtcu E, Erbek S, Atac FB, Sahin FI, and Cakmak O. Proinflammatory cytokine single nucleotide polymorphisms in nasal polyposis. *Arch Otolaryngol Head Neck Surg.* 2007;133(7):705-9.

150. Nichols DP, and Chmiel JF. Inflammation and its genesis in cystic fibrosis. *Pediatr Pulmonol.* 2015;50 Suppl 40:S39-56.
151. Lee RJ, Hariri BM, McMahon DB, Chen B, Doghramji L, Adappa ND, et al. Bacterial d-amino acids suppress sinonasal innate immunity through sweet taste receptors in solitary chemosensory cells. *Sci Signal.* 2017;10(495).
152. Lee RJ, Kofonow JM, Rosen PL, Siebert AP, Chen B, Doghramji L, et al. Bitter and sweet taste receptors regulate human upper respiratory innate immunity. *J Clin Invest.* 2014;124(3):1393-405.
153. Lee RJ, Chen B, Doghramji L, Adappa ND, Palmer JN, Kennedy DW, et al. Vasoactive intestinal peptide regulates sinonasal mucociliary clearance and synergizes with histamine in stimulating sinonasal fluid secretion. *FASEB J.* 2013;27(12):5094-103.
154. Lee RJ, Xiong G, Kofonow JM, Chen B, Lysenko A, Jiang P, et al. T2R38 taste receptor polymorphisms underlie susceptibility to upper respiratory infection. *J Clin Invest.* 2012;122(11):4145-59.
155. Freund JR, Mansfield CJ, Doghramji LJ, Adappa ND, Palmer JN, Kennedy DW, et al. Activation of airway epithelial bitter taste receptors by Pseudomonas aeruginosa quinolones modulates calcium, cyclic-AMP, and nitric oxide signaling. *J Biol Chem.* 2018;293(25):9824-40.
156. Hariri BM, McMahon DB, Chen B, Freund JR, Mansfield CJ, Doghramji LJ, et al. Flavones modulate respiratory epithelial innate immunity: anti-inflammatory effects and activation of the T2R14 receptor. *J Biol Chem.* 2017;292(20):8484-97.
157. Kreindler JL, Bertrand CA, Lee RJ, Karasic T, Aujla S, Pilewski JM, et al. Interleukin-17A induces bicarbonate secretion in normal human bronchial epithelial cells. *Am J Physiol Lung Cell Mol Physiol.* 2009;296(2):L257-66.
158. Hariri BM, McMahon DB, Chen B, Adappa ND, Palmer JN, Kennedy DW, et al. Plant flavones enhance antimicrobial activity of respiratory epithelial cell secretions against Pseudomonas aeruginosa. *PLoS One.* 2017;12(9):e0185203.
159. Hariri BM, Payne SJ, Chen B, Mansfield C, Doghramji LJ, Adappa ND, et al. In vitro effects of anthocyanidins on sinonasal epithelial nitric oxide production and bacterial physiology. *Am J Rhinol Allergy.* 2016;30(4):261-8.
160. Virgin FW, Rowe SM, Wade MB, Gaggar A, Leon KJ, Young KR, et al. Extensive surgical and comprehensive postoperative medical management for cystic fibrosis chronic rhinosinusitis. *Am J Rhinol Allergy.* 2012;26(1):70-5.
161. Groneberg DA, Peiser C, Dinh QT, Matthias J, Eynott PR, Heppt W, et al. Distribution of respiratory mucin proteins in human nasal mucosa. *Laryngoscope.* 2003;113(3):520-4.
162. Ianowski JP, Choi JY, Wine JJ, and Hanrahan JW. Substance P stimulates CFTR-dependent fluid secretion by mouse tracheal submucosal glands. *Pflugers Arch.* 2008;457:529-37.
163. Ianowski JP, Choi JY, Wine JJ, and Hanrahan JW. Mucus secretion by single tracheal submucosal glands from normal and CFTR knock-out mice. *J Physiol.* 2007;580:301-14.
164. Fischer H, Illek B, Sachs L, Finkbeiner WE, and Widdicombe JH. CFTR and calcium-activated chloride channels in primary cultures of human airway gland cells of serous or mucous phenotype. *Am J Physiol Lung Cell Mol Physiol.* 2010;299(4):L585-94.
165. Chiang L, Karvar S, and Hamm-Alvarez SF. Direct imaging of RAB27B-enriched secretory vesicle biogenesis in lacrimal acinar cells reveals origins on a nascent vesicle budding site. *PLoS One.* 2012;7(2):e31789.

166. Xu S, Edman M, Kothawala MS, Sun G, Chiang L, Mircheff A, et al. A Rab11a-enriched subapical membrane compartment regulates a cytoskeleton-dependent transcytotic pathway in secretory epithelial cells of the lacrimal gland. *J Cell Sci.* 2011;124(Pt 20):3503-14.
167. Hsueh PY, Edman MC, Sun G, Shi P, Xu S, Lin YA, et al. Tear-mediated delivery of nanoparticles through transcytosis of the lacrimal gland. *J Control Release.* 2015;208:2-13.
168. Edelstein A, Amodaj N, Hoover K, Vale R, and Stuurman N. Computer control of microscopes using microManager. *Curr Protoc Mol Biol.* 2010;Chapter 14:Unit14 20.
169. Wang KY, Arima N, Higuchi S, Shimajiri S, Tanimoto A, Murata Y, et al. Switch of histamine receptor expression from H2 to H1 during differentiation of monocytes into macrophages. *FEBS Lett.* 2000;473(3):345-8.
170. Triggiani M, Petraroli A, Loffredo S, Frattini A, Granata F, Morabito P, et al. Differentiation of monocytes into macrophages induces the upregulation of histamine H1 receptor. *J Allergy Clin Immunol.* 2007;119(2):472-81.